The Effect of Horizontal Pressure Gradients on the Momentum Transport in Tropical Convective Lines

By
Maria Flatau and Duane E. Stevens

Department of Atmospheric Science
Colorado State University
Fort Collins, Colorado

NSF ATM-8305759

Colorado State University

Department of Atmospheric Science

Paper No. 395

THE EFFECT OF HORIZONTAL PRESSURE GRADIENTS ON THE MOMENTUM TRANSPORT IN TROPICAL CONVECTIVE LINES

by

Maria Flatau

and

Duane E. Stevens

Research supported by the

National Science Foundation
under grant
ATM-8305759

Department of Atmospheric Science
Colorado State University
Fort Collins, Colorado

December 1985

Atmospheric Science Paper No. 395

Abstract

The Effect of Horizontal Pressure Gradients on the Momentum Transport in Tropical Convective Lines

Measurements of the momentum transport in tropical convective lines suggest that horizontal momentum can be generated on the cloud scale by the mesoscale low located near the center of the convective part of the line.

A simple convective parameterization is used to evaluate this effect. The parameterization is a version of the Fritsch and Chappell scheme modified for tropical conditions. Calculation of momentum is modified in order to evaluate the influence of the horizontal pressure gradients on momentum transport. The results suggest that in modeling of convective (particulary slow-moving) lines, horizontal pressure gradients should be taken into account. Sensitivity studies show that the magnitude of the calculated momentum flux strongly depends on average mesoscale vertical velocity and the vertical velocity in clouds.

The results from Fritsch and Chappell's parameterization are supported by the results of momentum flux calculations for the Lagrangian parcels moving in the two-dimensional pressure field generated by the slow moving convective lines. Some suggestions

concerning the proper formulation of the momentum flux parameterization are made.

Atmospheric Science Department
Colorado State University
Fort Collins, Colorado 80523
Fall 1985

ACKNOWLEDGEMENTS

We would like to thank Drs. Margaret LeMone, Richard Johnson and James Thomas for their reviews of this research and for helpful and inspiring discussions. We are also grateful to Dr. Johnson for presenting results of this study at the IAMAP/IAPSO conference.

We are deeply indebted to Dr. Gary Barnes from NCAR and to CSU students - Jen Luen Song, Craig Trembeck and Mel Nicholls for several useful conversations. We appreciate the support of the members of our research group. We are grateful to Annette Claycomb for editing and to Gail Watson for editing and typing the manuscript.

This work was sponsored by the National Science Foundation under grant ATM-8305759. Computing support was provided by the National Center for Atmospheric Research.

This paper is from a thesis submitted to the Academic Faculty of Colorado State University in partial fulfillment of the requirements for the degree of Master of Science.

I. Introduction

The properly formulated parameterization of convection is one of the most important problems in large- and mesoscale modeling. Because the strongest impact of convection on environment is connected with the release of latent heat, most convective parameterizations emphasize thermodynamic effects of cloud ensembles. However, dynamic effects of convection cannot be neglected. The first step towards formulation of parameterization of those effects is to determine the magnitude and structure of convective momentum fluxes through observation. This can be done by calculating the residual terms in large scale budget equations, but in the tropics the uncertainty in geopotential field measurements made this task practically impossible. However, substantial progress was made after the GARP Atlantic Tropical Experiment (GATE), which provided data with sufficient density and quality for momentum budget calculations.

The first attempt to calculate the momentum budget in tropical atmosphere was made by Stevens (1979). Using the data from Phase III of GATE (derived from A-scale and A/B-scale ship data), he calculated the vorticity, divergence, and momentum budgets for the average composite synoptic-scale wave. The results of this study showed the existence of the large apparent momentum sources in budget equations, suggesting that subsynoptic-scale circulations strongly affect wave dynamics. The momentum sources in Stevens' study were calculated as a

residual from the momentum equation for the synoptic wave, and geopotential was calculated from the hydrostatic equation and temperature field.

Another approach to the estimation of convective sources of momentum was presented by Sui (1984). He calculated vorticity residuals for seven convective events in GATE and then recovered momentum sources by integrating the Laplace equation:

$$\nabla^2 \left(\frac{\partial \psi}{\partial t} \right)_{cu} = Z$$

where Z is an apparent vorticity source and ψ the stream function. This approach, however, allowed him only to calculate the momentum source connected with a nondivergent part of the wind ($V_\psi = k \times \nabla \psi$).

As concluded by Stevens (1979), the apparent source of momentum has too complicated a structure to be parameterized by simple formulas like Rayleigh drag ($X = -D(p)u$) or diffusion ($X = K \frac{\partial^2 u}{\partial^2 z}$). Since an apparent source of momentum can be attributed to convective activity, a better way to parameterize this effect is to express it in terms of cumulus mass flux and the excess horizontal momentum of cumulus relative to the environment (Yanai, 1973; Schneider and Lindzen, 1976):

$$X = \sum_i \left[\sigma_i \omega_{ci} (V_{ci} - V_E) \right]_p \qquad (1.1)$$

where the summation is taken over all cloud types, σ_i is the fractional area occupied by each cloud type, ω is the vertical velocity in pressure coordinates ($m_i = -\sigma_i \omega_i$ is the mass flux in each cloud type), V_c, V_E represent horizontal velocity in cloud and in the environment respectively. As shown by Shapiro and Stevens (1980), eq. 1.1 can be written in the bulk form:

$$X = \delta\ (V_c - V_E) + [M_c V_{E,p} + \sigma\ (\nabla\phi)_c] \qquad (1.2)$$

In this formulation, the first term describes the detrainment of momentum to the environment (δ is the detrainment coefficient), $M_c V_E$ describes the effects connected with compensating environmental subsidence caused by the convective activity, and $\sigma(\nabla\phi)_c$ describes the changes caused by the horizontal acceleration in clouds caused by cloud-scale horizontal pressure gradients. A one-dimensional cloud model is used to calculate V_c, M_c and δ. The term involving cloud-scale pressure gradients is usually neglected.

The formula (1.2) was used by Shapiro and Stevens (1980) to calculate convective momentum fluxes, in order to compare them with the apparent momentum sources from Stevens' (1979) large-scale momentum budget calculations. The results showed some inconsistencies between parameterized and observed convective momentum sources, although the same comparison for vorticity showed much better agreement. Shapiro and Stevens concluded that the momentum fluxes can be much more dependent on organization of the convective system than vorticity fluxes. The assumption that the influence of the cloud-generated pressure forces on momentum flux is negligible can be justified in the case of strictly random convection, but it is questionable for the highly organized convective systems such as convective lines.

Indeed, aircraft measurements of momentum flux in GATE convective lines documented by LeMone (1983)and LeMone et al. (1984) suggested that although the momentum fluxes for the isolated clouds or less-organized convective lines do not show the influence of pressure

gradients, the momentum flux in two-dimensional convective lines is strongly affected by the horizontal pressure gradient force. In GATE, the fluxes of horizontal momentum perpendicular to the line were always negative (when positive horizontal wind is in the direction of line motion), showing in many cases the upgradient transport of momentum. LeMone et al. (1984) argued that taking into account this kind of momentum transport in the convective lines observed in GATE would improve Shapiro and Stevens (1980) results and bring parameterized values of apparent momentum sources closer to those calculated from large-scale budget.

LeMone's observational results were supported by the results of the numerical study of the momentum generation in the tropical convective line, presented by Soong and Tao (1984). They used a two-dimensional cloud ensemble model to simulate the formation of an ensemble of clouds under the given large scale conditions. The momentum flux perpendicular to the line ($\overline{u'w'}$) appeared to be extremely sensitive to the details of simulations, as was the cloud configuration produced by the model. Since the momentum flux in the direction parallel to the line ($\overline{v'w'}$) remained almost unchanged, they concluded that it was the pressure force connected with the cloud configuration that caused such dramatic changes in the u-momentum flux.

The results presented by LeMone (1983) and LeMone et al. (1984) showed also that most of the momentum generation occurs in the convective part of the line - the narrow (20-40 km) zone behind the leading edge. This suggests that convection-generated pressure forces can cause problems not only in large-scale models, but also in

mesoscale models. However, the convective parameterization used in mesoscale models also use the assumption that horizontal momentum in clouds is conserved (Raymond 1984, Beniston 1985, Fritsch and Chappell 1980 a,b). It is the goal of this study to determine, using the data from the GATE two-dimensional convective lines and simple convective parameterization, what error can be made by neglecting the cloud-scale pressure forces in parameterization of convective momentum flux. We evaluate the effect of horizontal pressure forces on momentum flux using two methods. In the first, we use the convective parameterization designed by Fritsch and Chappell, but modified for tropical conditions. This procedure is described in Chapter II, and the results appear in Chapter III. Chapter IV describes the other approach we used. In this part we calculate the momentum fluxes for the set of Lagrangain parcels moving in the two-dimensional pressure field generated by the convective line. The conclusions are contained in Chapter V. The Appendix A contains some of our suggestions concerning implementation of the Fritsch and Chappell parameterization in mesoscale models.

II. Description of the Fritsch and Chappell Parameterization

In numerical models momentum fluxes generated by convection are usually parameterized with the formula 1.1.

The cloud budget of the horizontal momentum is given by:

$$\frac{\partial}{\partial z}(M_c u_c) + \delta u_c - \varepsilon u_E = -\sigma \nabla p = F_c \qquad (2.1)$$

where ε and δ are entrainment and detrainment coefficients, σ is the area occupied by convection and F_c is the horizontal pressure force The purpose of this study is to determine, using convective parameterization and data for the convective lines studied by LeMone et al. (1984), the change in momentum flux caused by horizontal pressure forces acting on updraft and downdraft parcels. Since we deal with mesoscale phenomena, where convective drafts can occupy a significant fraction of the grid area, we chose the Fritsch and Chappell (1980a) parameterization, which was designed for mesoscale models with grid spacing about 20 km and which does not contain the assumption that the area occupied by active convection has to be small.

2.1 General description

The Fritsch and Chappell parameterization is based on a local consumption of the available buoyant energy. In this parameterization the mesoscale model provides temperature, humidity, and horizontal and vertical velocities at the given grid point. If the mesoscale model

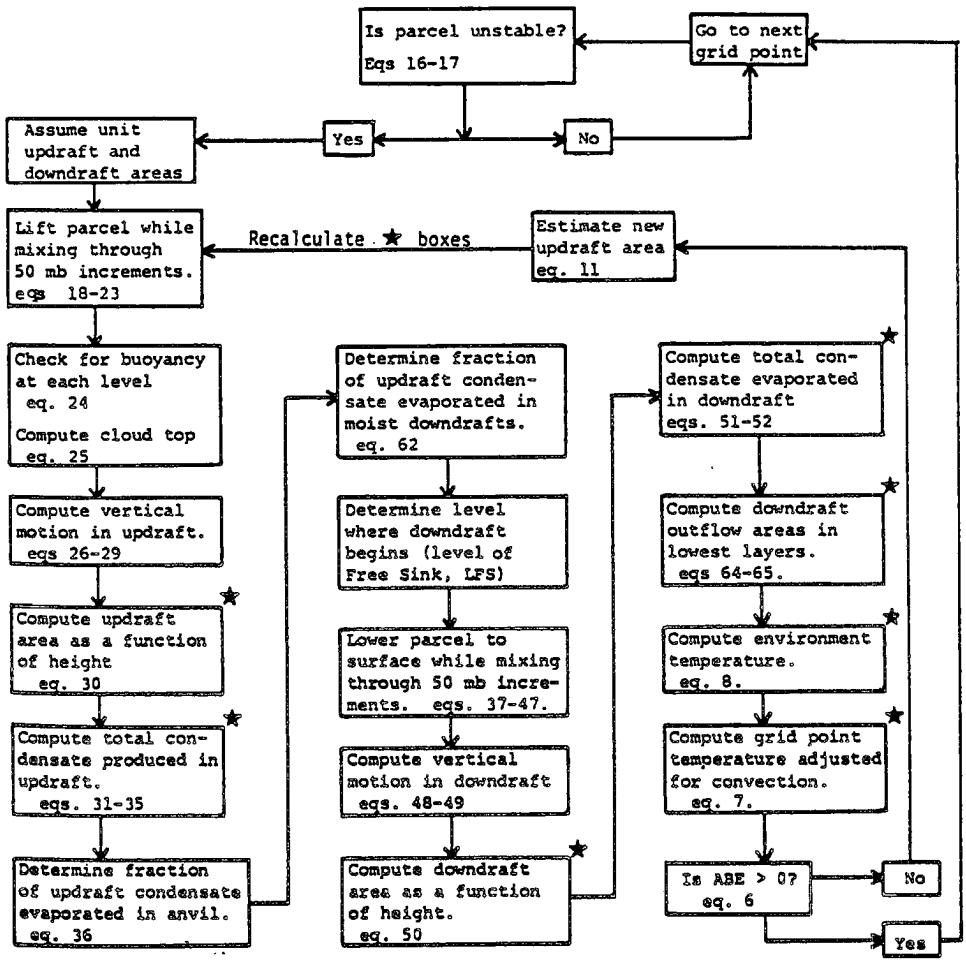

Fig. 2-1 Flow diagram for the Fritsch and Chappel parameterization.

generates positive available buoyant energy at this grid point, convection is assumed to entirely remove this energy in the specified period of time τ_c. A simple one-dimensional cloud model is used to calculate vertical distributions of the temperature, mixing ratios, and momentum adjusted for convection.

To determine the amount of convection (updraft and downdraft area) the following iterative procedure is used: Initially it is assumed that updraft occupies 1% of the grid area. Temperature, water vapor mixing ratio, and the amount of condensate are calculated for the updraft and downdraft. The amount of downdraft air corresponding to the initial unit of updraft air is determined (see next section). Environmental compensating subsidence is calculated from the mass continuity condition. The new values of variables in the considered grid area are evaluated as the average over updraft, downdraft, and environment area. If the new buoyant energy is larger then zero, a larger area of the updraft is assumed, and the calculation is repeated. This iterative procedure is continued until all buoyant energy is used for convection. Final values of meteorological parameters adjusted for convection are used to calculate convective tendencies in the mesoscale model. A flow diagram for the parameterization and its interaction with the mesoscale model is shown in Fig. 2-1.

Fritsch and Chappell's parameterization was originally designed for mid-latitudes and involves a large number of specified a priori parameters based on mid-latitude experiments. In our calculations the basic idea of Fritsch and Chappell's parameterization is preserved, but parameters more appropriate for tropical conditions are used. Also,

horizontal pressure gradient terms are introduced in calculations of the horizontal momentum perpendicular to the line.

2.2 Mesoscale conditions

The mesoscale conditions needed as input to the Fritsch and Chappell parameterization are: vertical profiles of temperature, mixing ratio and horizontal wind used as initial environmental values; and vertical profile of mesoscale vertical velocity to calculate compensating subsidence. Usually mesoscale values are provided by a mesoscale numerical model. However, in this study we use the GATE observations for the quasi two-dimensional convection line, rather than a numerical model, to supply the input values for the parameterization. Composite soundings for the environment of the fast and slow convective lines and environmental horizontal wind profiles are shown in Fig. 2-2. We use a right-handed coordinate system in which axis X is normal to the line with positive sign in the direction of the line movement, and axis Y is parallel to the line. Pressure disturbance fields for those lines appear in Fig. 2-3. Horizontal pressure gradients in the Y direction are equal to zero. Due to the lack of data above 6 km we assume that pressure forces above this level are also equal to zero. We perform our calculations for the convective part of the line. According to Barnes and Sieckman (1984), the convectively active region of the line occupies roughly a 20-40 km wide zone normal to the leading edge. For the purpose of our calculations, we define the convective part of the line as the first 30 km behind the leading edge. Fig. 2-4 shows the virtual temperature disturbance field calculated from the pressure disturbance field shown

a

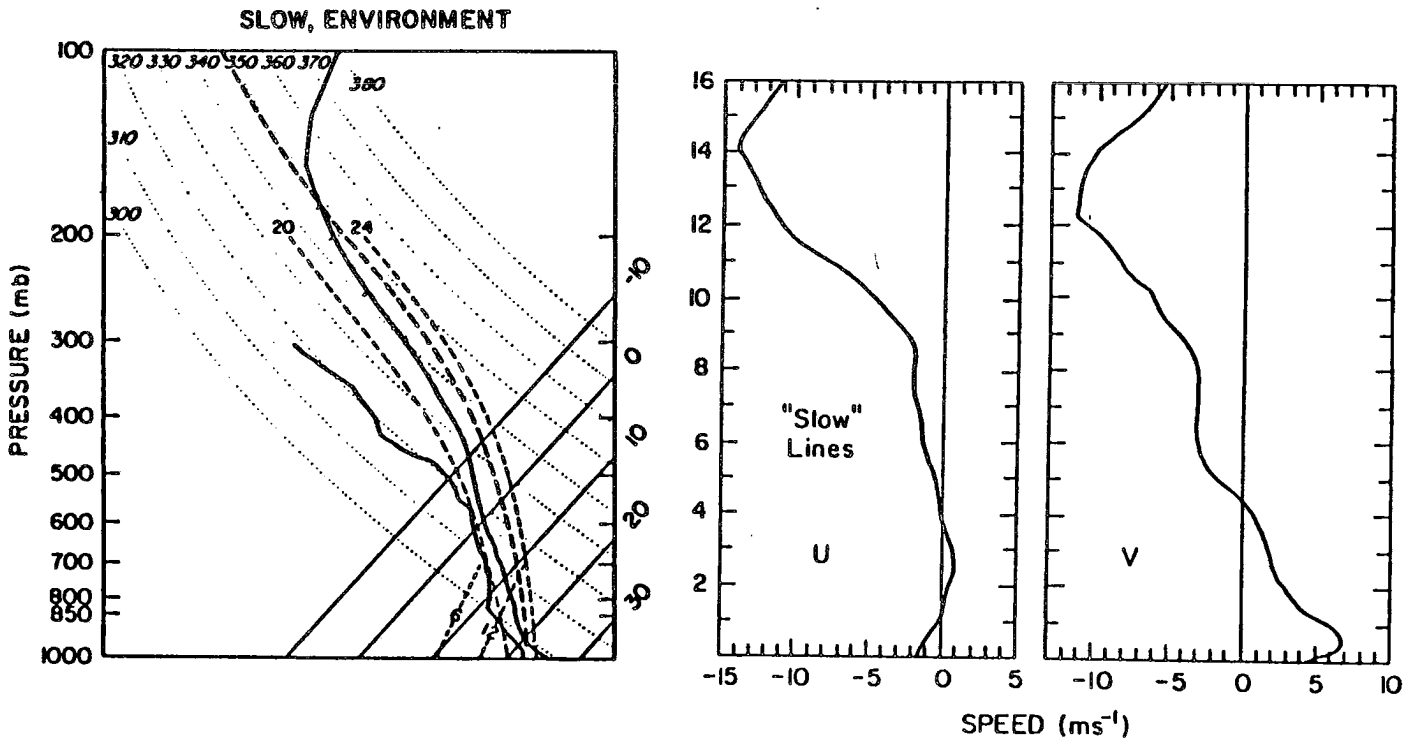

Fig. 2-2 Composite environmental sounding and horizontal wind used in the parameterization a/for the slow line b/for the fast line (Barnes, 1984).

b

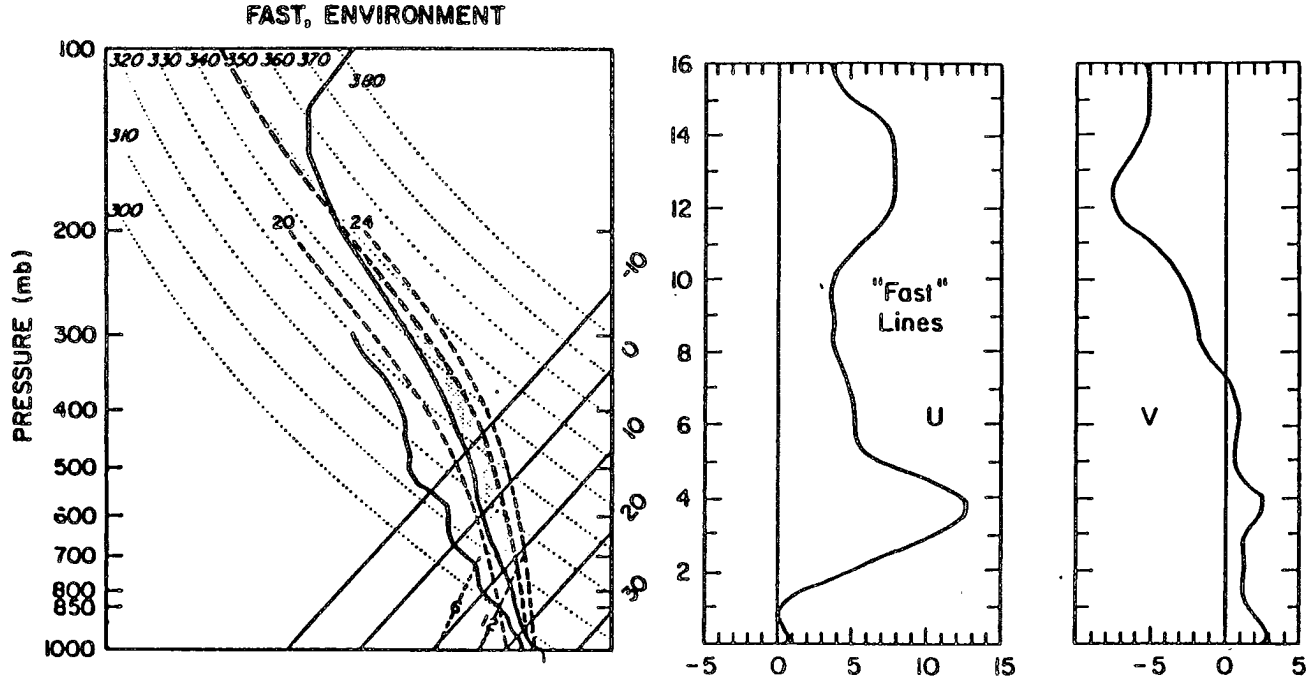

Fig. 2-2 (continued)

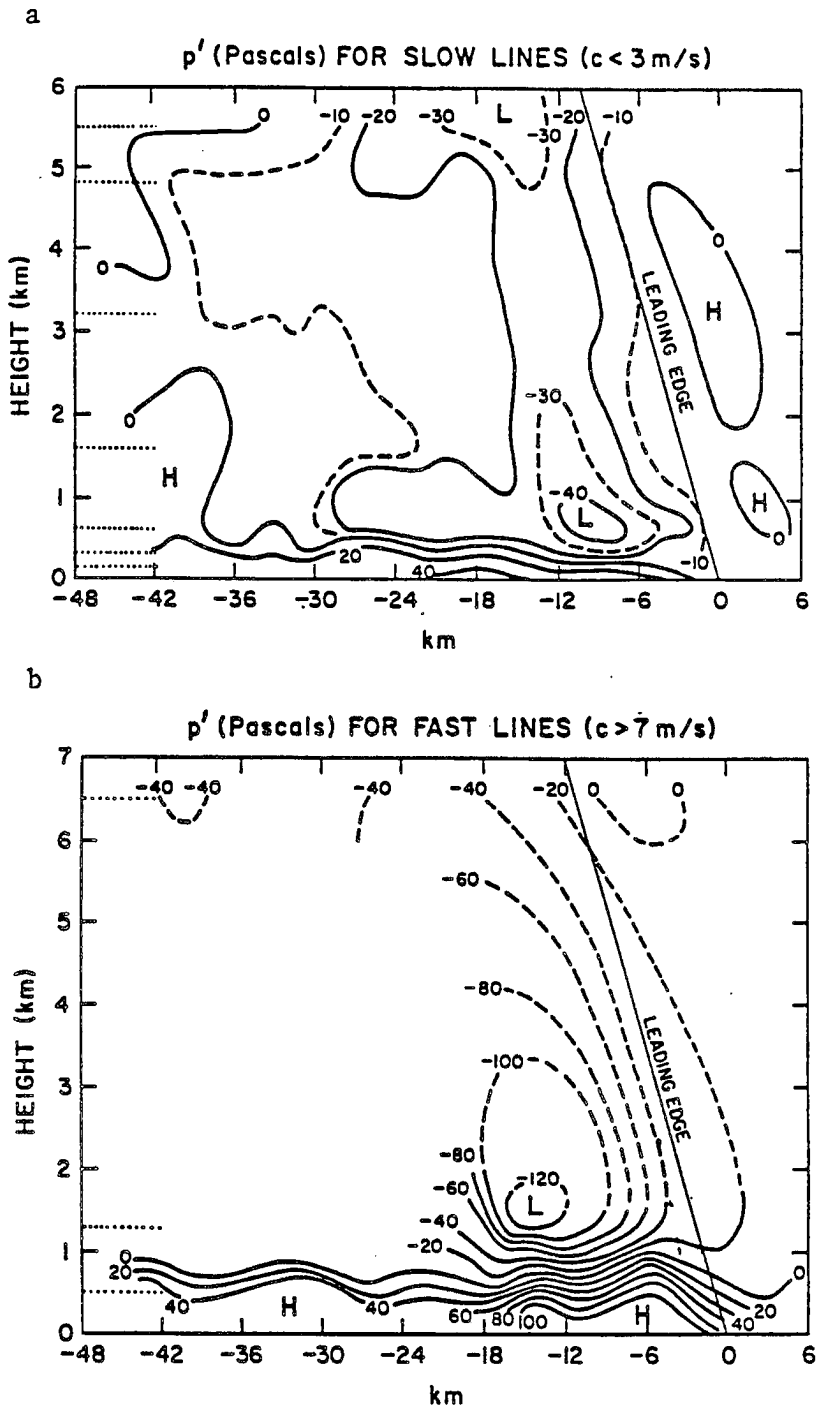

Fig. 2-3 Composite pressure disturbance field for the a/ slow b/fast GATE convective lines (LeMone, 1984).

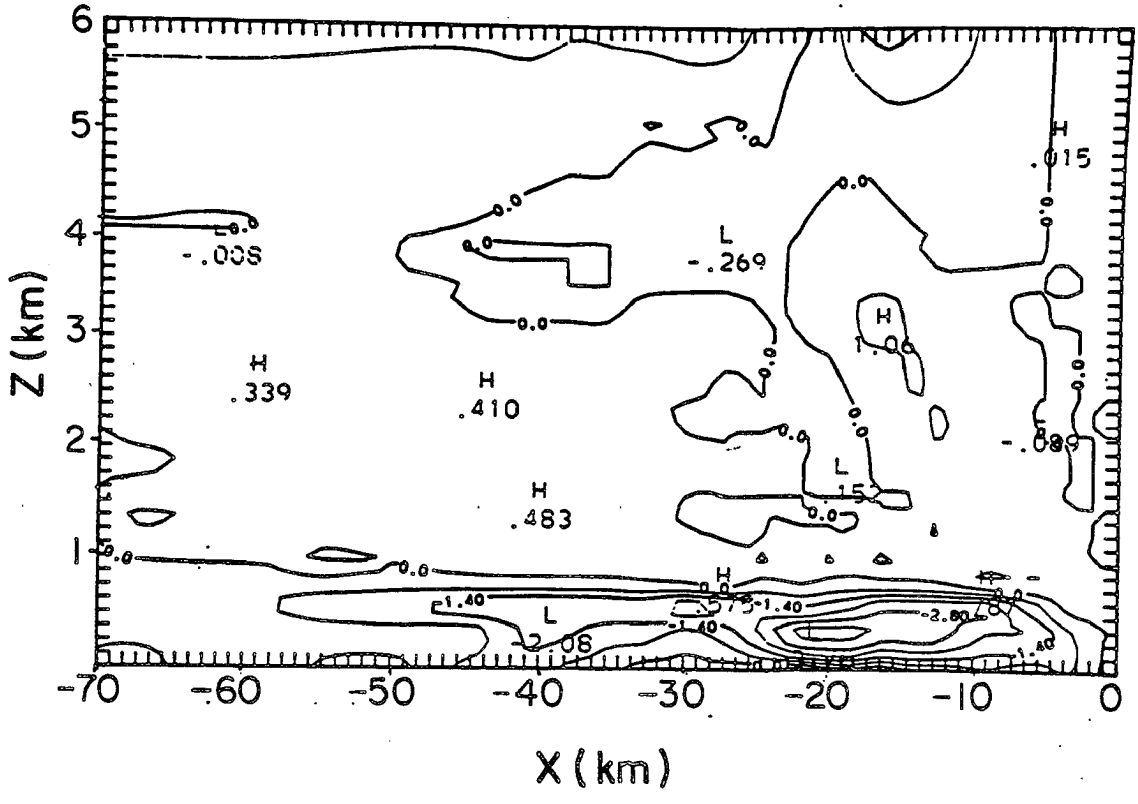

Fig. 2-4 Disturbance of the virtual temperature, calculated from the hydrostatic equation and the pressure disturbance field shown on Fig. 2-3a.

in Fig. 2-3a, with the assumption that pressure disturbance is hydrostatic. The greatest temperature changes (strong heating in the upper layers close to the leading edge and strong cooling on the surface) occur in the convective region. Barnes and Sieckman's (1984) calculations also show that the buoyant energy is significantly reduced (96% in the fast composite line and 66% in the slow composite line) in the convective part of the line. Because we do not take into account the differences in the size of convective area, we assume for both types of lines that 80% of the initial convective energy is removed in the 30 km wide convective region. This implies that the time required by convection to remove buoyant energy is calculated as $\Delta x/c$, where c is the speed of the line known from observations and Δx = 30 km. When the Fritsch and Chappell parameterization is used in the mesoscale model (Fritsch and Chappell, 1980a, 1980b) τ_c is estimated as the time needed for clouds to move through the grid element, by dividing grid length by the mean environmental wind speed.

In order to evaluate compensating subsidence in the environment, it is necessary to know the mean vertical velocity in the considered grid area. This mesoscale vertical velocity is usually provided by the mesoscale model. In our study we assume that the average vertical velocity is equal to zero, but "average vertical velocity" means in this case vertical velocity averaged over an area larger than our "grid box", because it would not be reasonable to assume that mean vertical velocity in the convective part of the line is equal to zero. This means that we allow compensating subsidence to occur outside the convective region. We also run parameterization with different mesoscale vertical velocities in order to evaluate the sensitivity of calculated momentum fluxes to this parameter.

According to LeMone (1983), the updraft cores tend to occur between the leading edge and the pressure low, and downdraft cores are observed behind the low. (Fig. 2-5). Therefore, in this study pressure gradient forces acting on updraft and downdraft cores are assumed to have opposite signs. Since the center of the low pressure is close to the center of the considered region, pressure forces acting on the cores are stronger than those for environmental parcels.

2.3 Cloud model

The one dimensional cloud model used in the Fritsch and Chappell parameterization consists of a steady-state plume convective updraft and a steady state plume convective downdraft. It is assumed that the mass of the updraft changes linearly from the cloud base to the cloud top, so the fractional entrainment for a layer is equal to:

$$\Delta K_u(k) = B_u \, [z(k+1) - z(k)] \, / \, [z_{CT} - z_{LCL}] \qquad (2.3)$$

where $\Delta K_u(k)$ is the amount of entrained mass for the level $z(k)$; B_u is a constant depending on how much mass is entrained between the cloud base and the cloud top; z_{LCL} is the height of the cloud base and z_{CT} is the height of the cloud top. A similar procedure is used for the downdraft which increases its mass from the level of free sink to the surface. Detrainment is neglected for both updraft and downdraft. To initialize the updraft, 50 mb layers are mixed and checked for buoyancy on the lifting condensation level (LCL). The lowest layer buoyant on its LCL is chosen as the cloud base. The downdraft starts at the level where a 1:1 mixture of updraft air and environmental air becomes negatively buoyant.

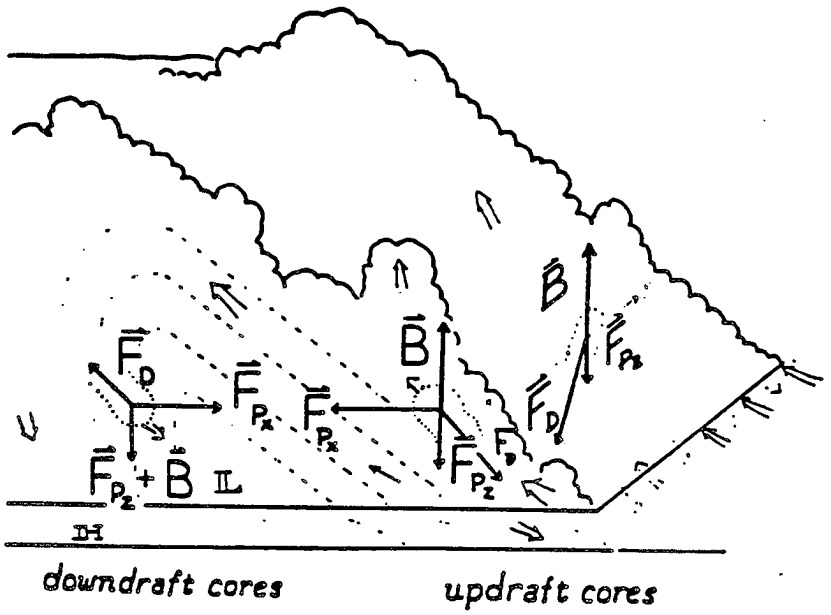

Fig. 2-5 Schematic of the processes leading to momentum generation in the convective band (LeMone, 1983).

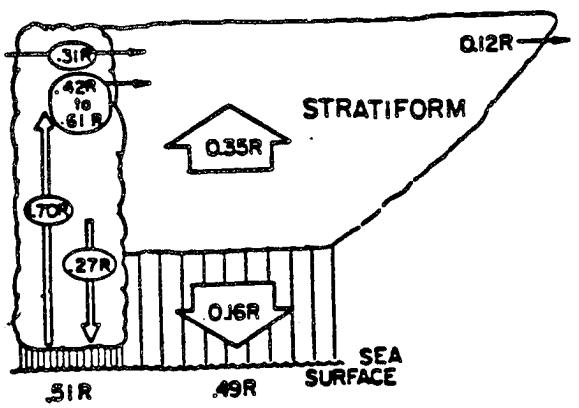

Fig. 2-6 Schematic diagram of the squall-system water budget (Gamache and Houze, 1983).

The cloud top is defined as the level where vertical velocity in the updraft becomes negative. In the original Fritsch and Chappell formulation, vertical velocity in updraft and downdraft depends only on buoyancy force. In our study, following Anthes (1977) liquid water drag (only in the updraft), virtual mass effect (see Appendix B), and mixing of the vertical momentum are also taken into account. The temperature of the updraft changes due to adiabatic cooling, diabatic heating (condensation and freezing), and mixing with the environment. Downdraft temperature is changed by adiabatic warming, mixing, melting, and the evaporation of the condensate. It is assumed that the downdraft is always saturated above the cloud base. Condensate in the updraft freezes at -5°C, and melting level for downdraft is at 0°C.

Fritsch and Chappell calculate a fraction of the condensate evaporated in the anvil and lost by precipitation. Those calculations give the basis for determining the area occupied by a downdraft relative to the updraft area. They assume that all condensate that did not evaporate in the anvil and did not reach the ground evaporates in the downdraft. Since evaporation per unit area in the downdraft can be calculated, it is possible to determine the downdraft area needed to satisfy this condition. The same approach is taken in our study, but the ratio of the water condensed in updraft to the water evaporated in downdraft is taken from the Gamache and Houze (1983) observational study of convective systems in GATE (Fig. 2-6).

Horizontal momentum in updrafts and downdrafts is changed by entrainment of the environmental momentum and by horizontal pressure gradients (eq. 2.1).

Changes in the environment are caused mainly by compensating subsidence. Temperature and mixing ratio of the environment can also change because of evaporation of the condensate in the anvil (anvil is defined by Fritsch and Chappell as the region from the equilibrium level to the cloud top). Grid point values adjusted for convection are defined as:

$$X(z) = A^{-1} [X_E(z)\, A_E(z) + X_D(z)\, A_D(z) + X_U(z)\, A_U(z)] \qquad (2.4)$$

where $X(z)$ is the value adjusted for convection, subscripts E, D, U identify environment, downdraft, and updraft respectively, and $A = A_E + A_D + A_U$ is the grid element area.

III. Analysis of the Results

Vertical fluxes of the horizontal momentum depend on cloud mass flux, wind shear, pressure forces, and vertical velocity in updraft (downdraft) which determines the time in which the pressure gradient force can act on updraft (downdraft) parcels (eq. 2.2). In the first section of this chapter we will present the influence of the horizontal pressure gradients on the momentum flux in the slow- and fast-moving convective lines. In this section, for both types of lines, we use the condition that the mesoscale vertical velocity is constant with height and equal to zero. Compensating subsidence is allowed to occur on an area four times larger than the area at the convective region. In the second section we will compare our results with GATE observations, and discuss factors influencing cloud mass flux (e.g., assumptions concerning mesoscale vertical velocity), which in turn determines the magnitude of the momentum flux. In the third section we will consider what implications our findings can have for mesoscale numerical models.

3.1 The influence of the horizontal pressure gradients on the momentum flux.

As we mentioned before, the influence of the horizontal pressure force on the momentum of the updraft (downdraft) parcels depends on the vertical velocity in the updraft (downdraft). The vertical

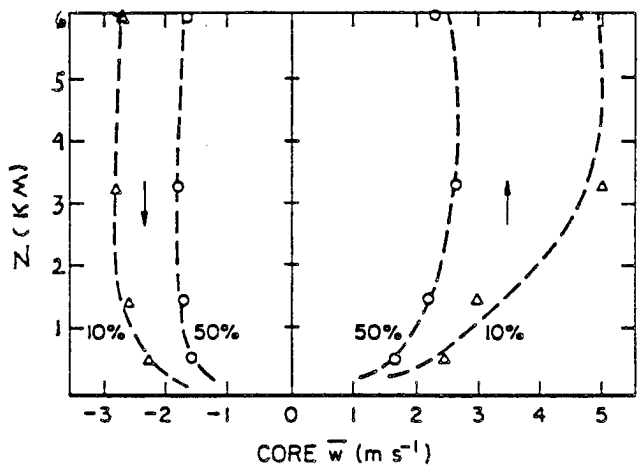

Fig. 3-1 Vertical velocity in the GATE convective cores (LeMone and Zipser, 1980).

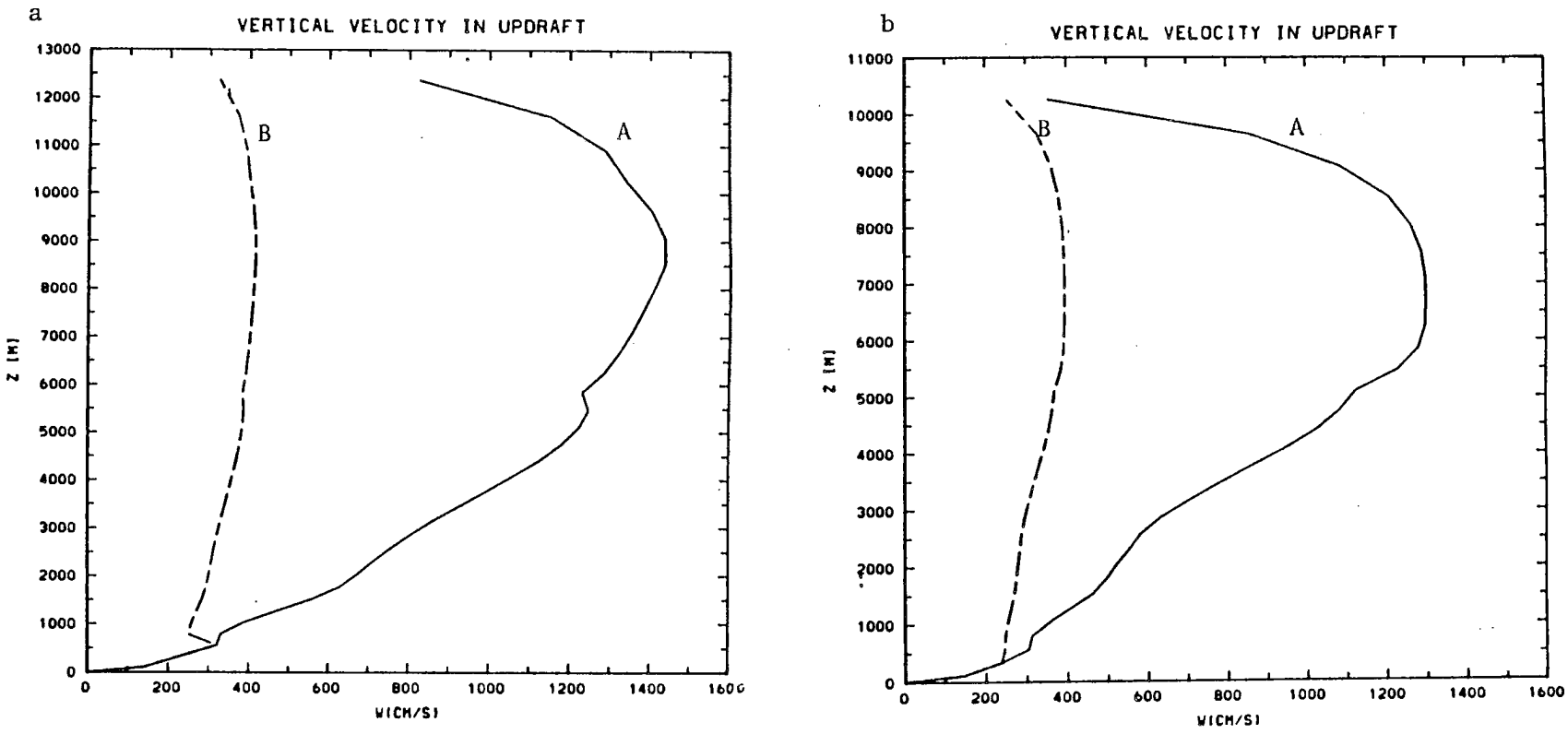

Fig. 3-2 Vertical velocity in updraft: A - calculated from vertical momentum equation; B - modified to match GATE data; a/ for the slow convective line, b/ for the fast convective line.

velocities calculated in Fritsch and Chappell parameterization reach 15 m/s, and they are much too large compared with vertical velocities measured in the GATE convective cores which, as can be seen from Fig. 3-1, have the median value about 2 m/s. A similar problem was reported by Zipser and LeMone (1980). Despite the use of different models, different soundings, and different mesoscale conditions they were not able to obtain realistic vertical velocities and realistic cloud top heights at the same time. Zipser and LeMone (1980) attribute this difference to the fact that the "environment" of the convective cores is defined not by the sounding ahead of the convective line but by the mesoscale conditions.

Because of this large difference between calculated and measured vertical velocity in clouds, we performed two sets of experiments. In the first set, we used vertical velocities calculated in the parameterization; in the second, the cloud vertical velocities were modified to match approximately the vertical velocities observed in the GATE convective cores (Fig. 3-2), while keeping the mass flux as calculated in the parameterization. The results for the slow and fast convective line are shown in Figs. 3-3 to 3-6. Fig. 3-3 a,b show the area occupied by convective updrafts for the slow and fast convective line. In the Fritsch and Chappell parameterization the area of the convective draft is calculated as:

$$\delta = M_c/(w \cdot \rho)$$

where the mass flux (M_c) and vertical velocity (w) in convective drafts are calculated independently. This implies that the area occupied by convection is much larger when we use the vertical

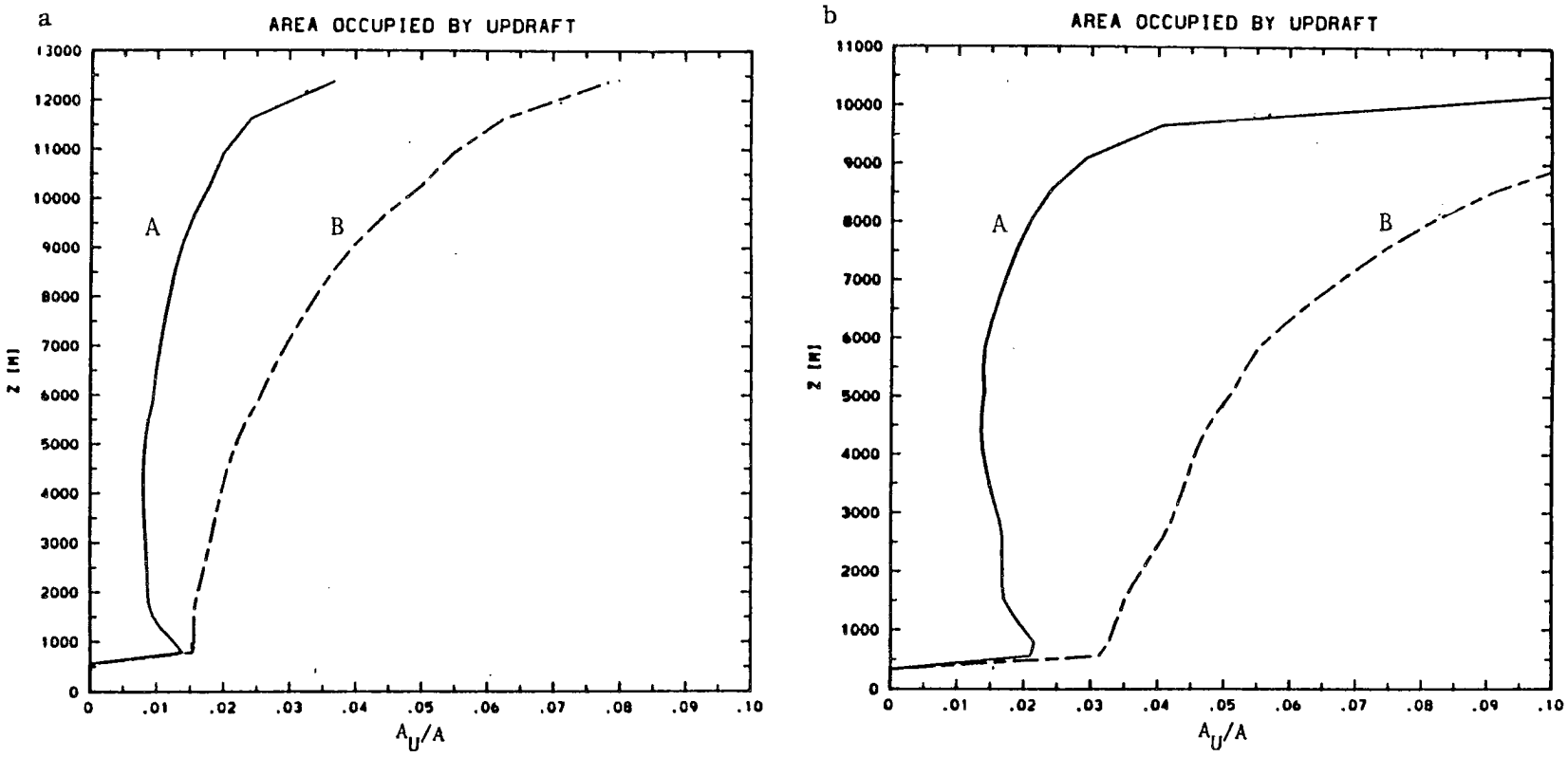

Fig. 3-3 Fraction of the grid area occupied by the updraft calculated with: A - calculated vertical velocity; B - observed vertical velocity; a/ for the slow convective line, b/ for the fast convective line.

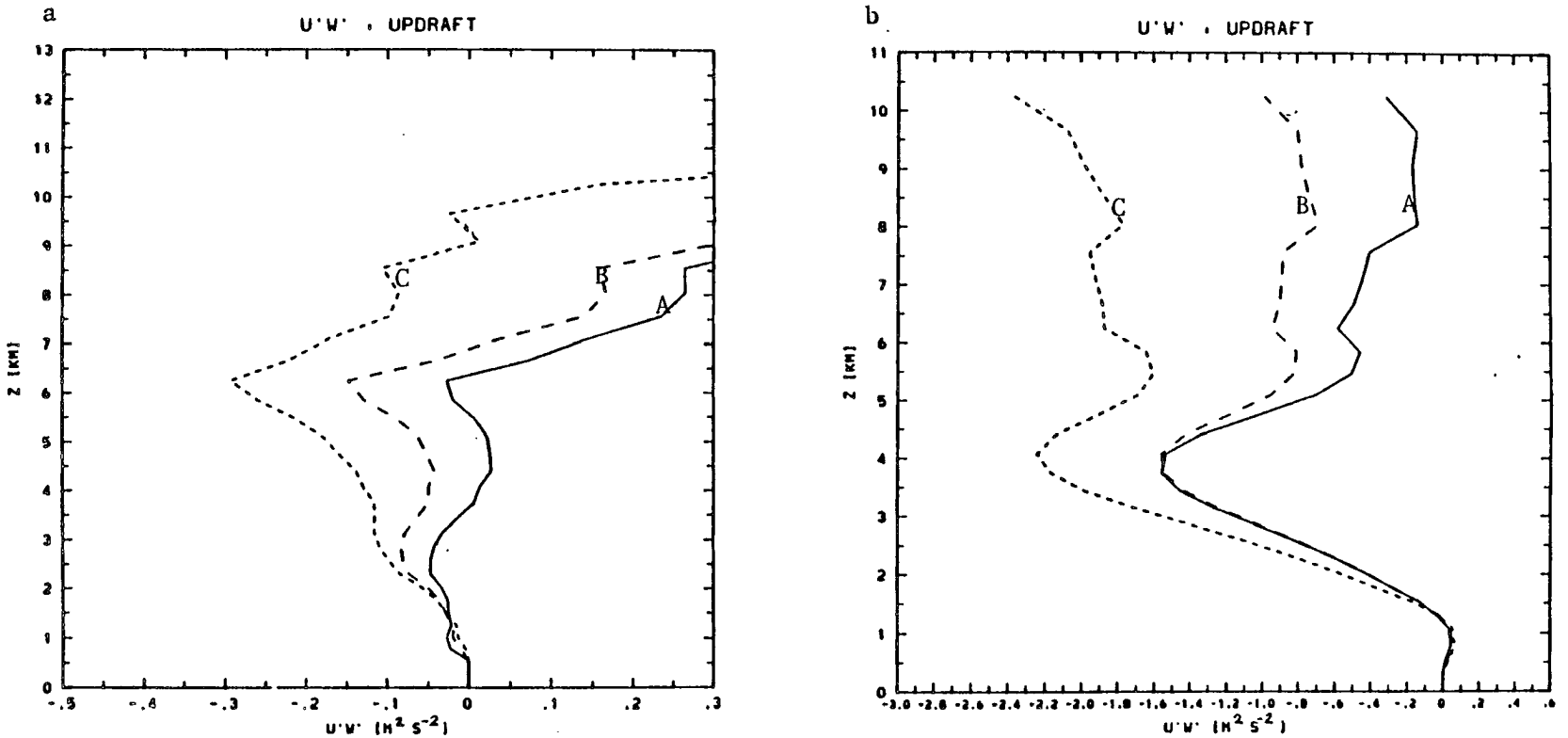

Fig. 3-4 Horizontal momentum flux u'w' due to the updraft: A - calculated without horizontal pressure forces, B - with vertical velocity in updraft calculated in parameterization and horizontal pressure gradient forces, C - with vertical velocity in updraft from observations and horizontal pressure gradient forces; a/ in the slow-moving line, b/ in the fast-moving line.

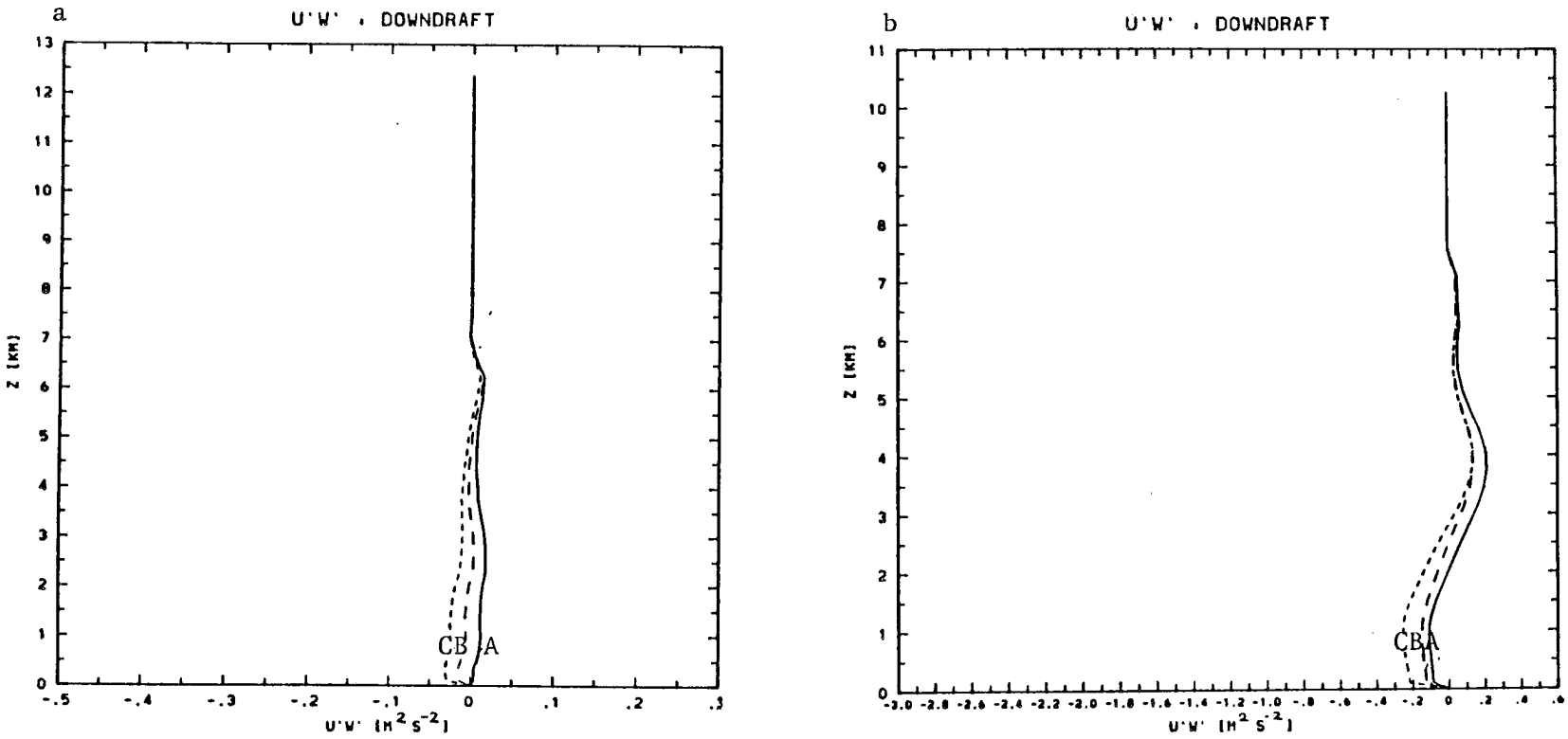

Fig. 3-5 Horizontal momentum flux $\overline{u'w'}$ due to the downdraft: A - without horizontal pressure force, B with horizontal pressure force and vertical velocity in downdraft calculated in the parameterization, C - with the horizontal pressure force and observed vertical velocity in downdraft; a/ in the slow-moving line, b/ in the fast-moving line.

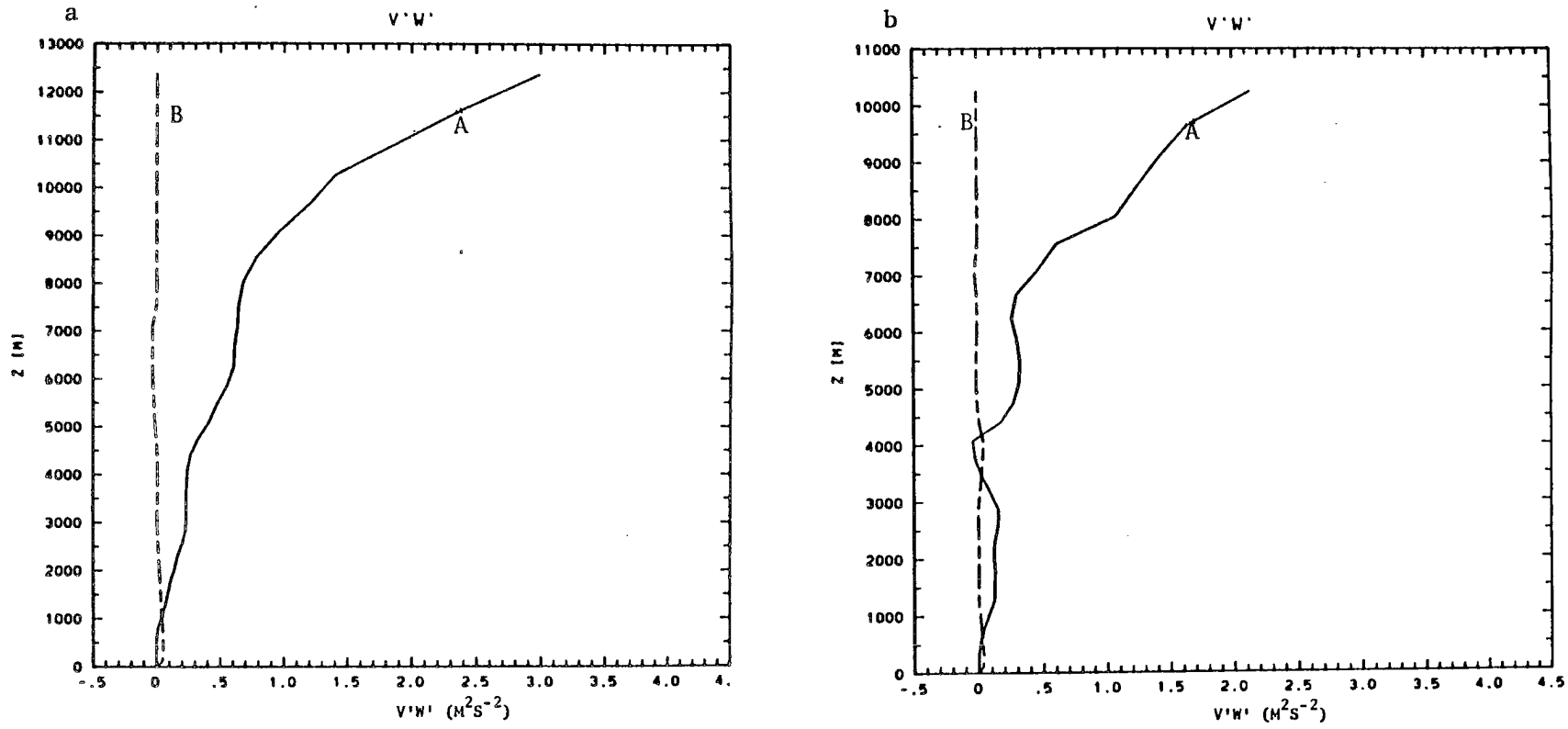

Fig. 3-6 Horizontal momentum flux v'w': A - generated by updraft, B -generated by downdraft; a/ in the slow-moving line, b/ in the fast moving line.

velocities in drafts from GATE measurements. Since the vertical velocities are similar for both types of lines (Fig. 3-2), Fig. 3-3 indicates also that mass flux in the fast convective line is about 2.5 times larger than in the slow line.

Figs. 3-4 and 3-5 show the momentum fluxes produced by the updraft (Fig. 3-4) and downdraft (Fig. 3-5) for three cases. In the first case (indicated by line A) the horizontal pressure forces are neglected. In the second case (line B) the horizontal drafts calculated in the parameterization is used. In the third case horizontal pressure gradients and vertical velocities from GATE are used. Comparison of Fig. 3-4 and 3-5 shows that for both types of lines the momentum flux generated by the downdraft is about an order of magnitude smaller than the momentum flux generated by the updraft. This result is caused by a similar difference in the mass fluxes for the updraft and downdraft. As described in Chapter II, the mass flux in the downdraft is estimated from the water budget considerations. Because the slow-moving lines are roughly aligned to maximize the vertical shear parallel to their axes (LeMone et al., 1984, Fig. 2-2a), $\overline{u'w'}$ (Fig. 3-4a) without horizontal pressure forces is much smaller than $\overline{v'w'}$ (Fig. 3-6a) and changes sign according to the changes in the environmental wind. When the pressure gradient forces are taken into account, momentum flux $\overline{u'w'}$ becomes larger and negative. This effect is about two times stronger when we consider vertical velocities matching those for GATE convective cores.

The momentum flux for the fast line (Fig. 3-4b) is about ten times bigger than for the slow one. This can be explained by the presence of the larger mass flux and stronger shear in the u velocity.

Horizontal pressure gradients in the fast convective line are stronger than those in the slow line, and also act to increase the magnitude of the momentum flux, but they do not significantly change the shape of the momentum flux profile, as in the case of the slow line. Because in the fast line low-level shear in the horizontal wind parallel to the line is small, $\overline{v'w'}$ momentum fluxes (Fig. 3-6b) below 6 km are smaller than $\overline{u'w'}$ and have magnitudes similar to those in the slow line (3-6a).

These results show that the change of momentum flux caused by horizontal pressure gradient depends strongly on vertical velocity in clouds. Therefore, to account properly for the effect of the horizontal pressure, it is necessary to use a parameterization which produces realistic vertical velocities.

Most interesting from the modeling point of view are vertical derivatives of the momentum fluxes. They are shown in Fig. 3-7. The derivative of the momentum flux in the fast line (Fig. 3-7 b) is about ten times larger than in the slow line (Fig. 3-7 a). A comparison of the vertical derivative of the momentum flux calculated with (lines B, C) and without (line A) pressure gradients for both types of lines indicates that momentum flux derivative shows relatively less dependence on pressure gradient, for the fast line. The maximum change caused by taking into account horizontal pressure gradient (i.e., C-A) is, in the case of slow line, of the same magnitude as the vertical derivative of the momentum flux calculated without pressure gradients (Fig. 3-7 a, line A). In the case of fast line it is about three times smaller than the momentum flux derivative.

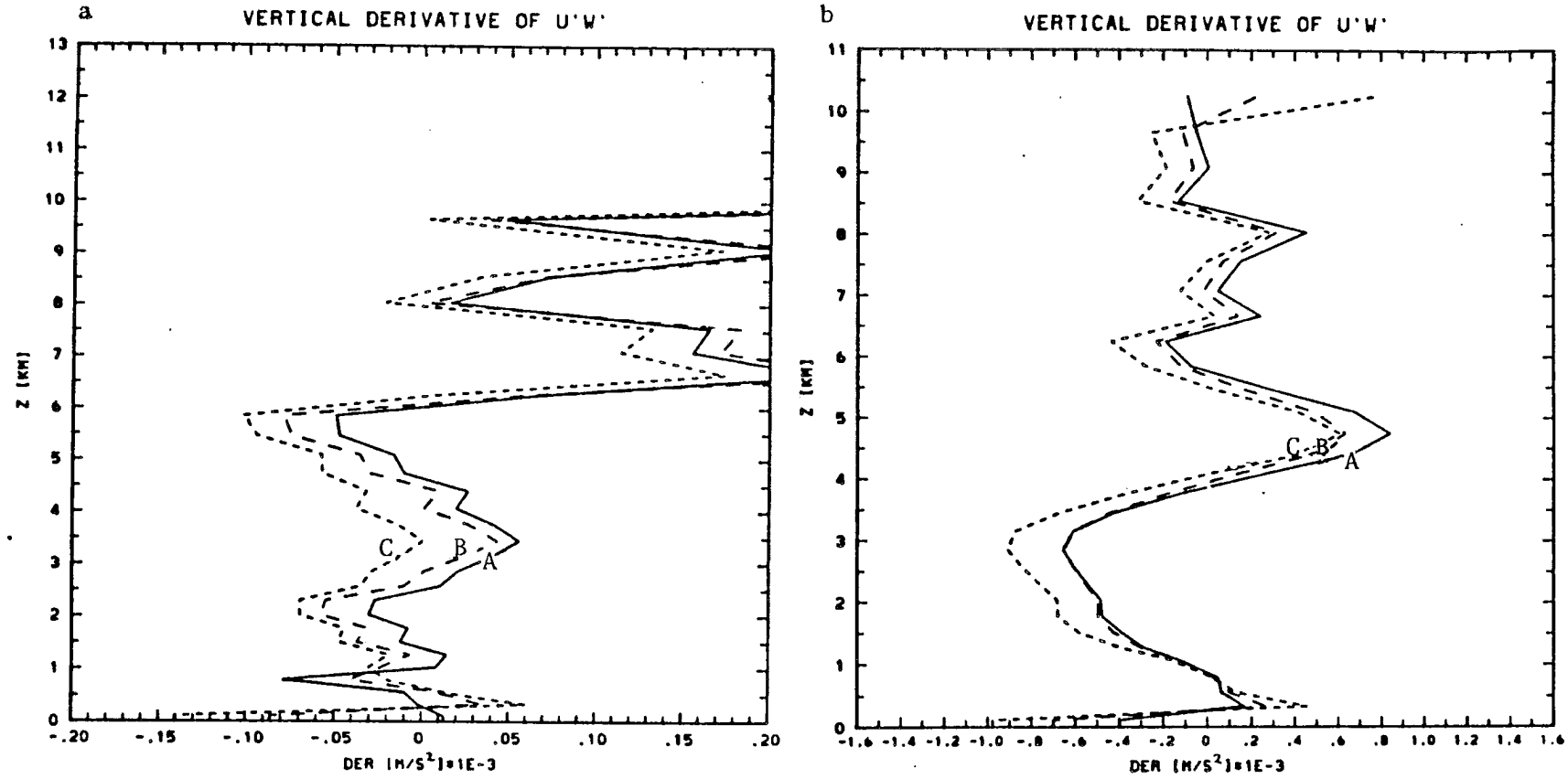

Fig. 3-7 Vertical derivative of the horizontal momentum flux; A - calculated without horizontal pressure gradients; B, C, with pressure gradients and vertical velocity in updraft and downdraft, B - calculated, C - observed; a/ in the slow-moving line, b/ in the fast-moving line.

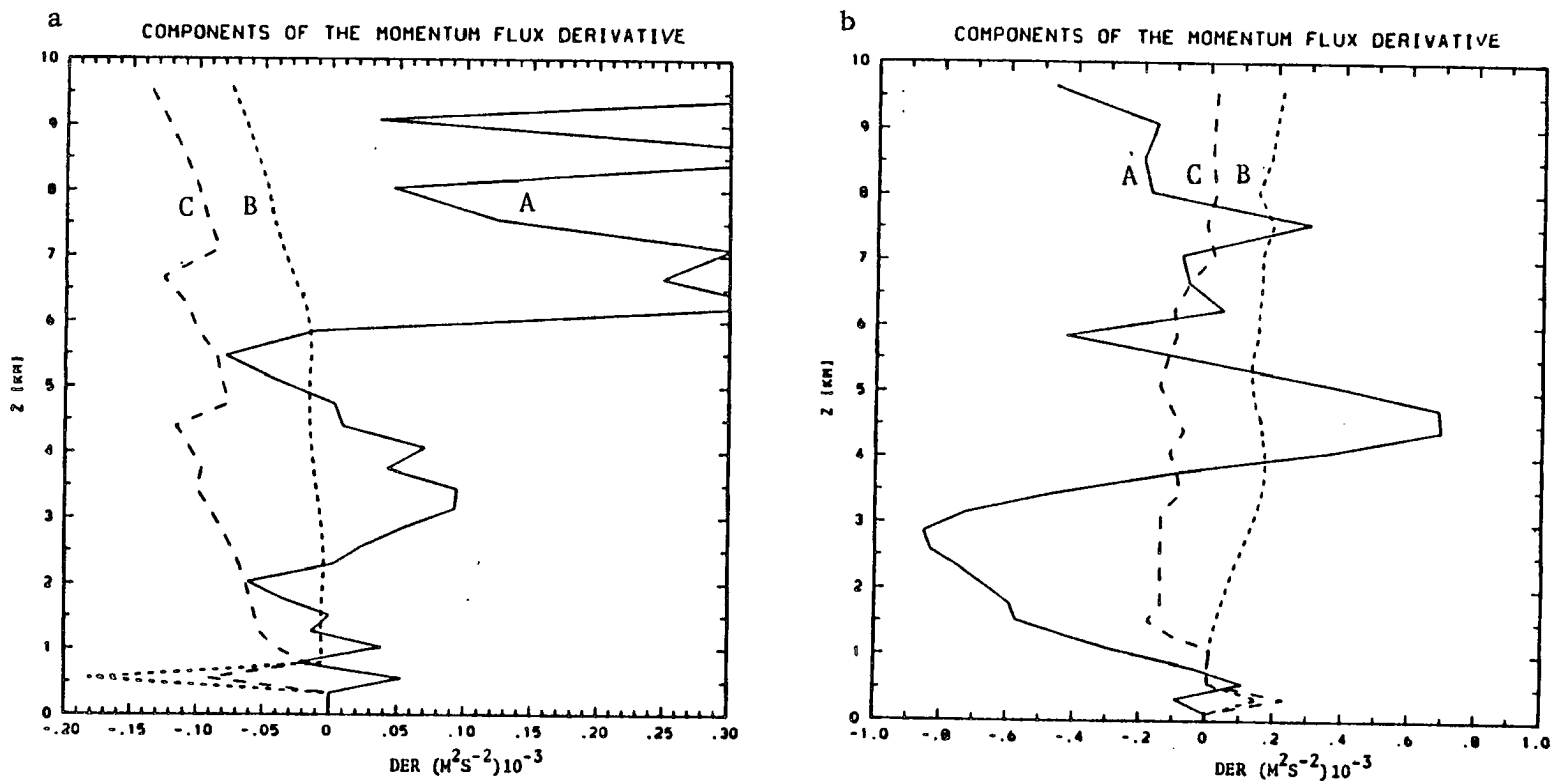

Fig. 3-8 Components of the momentum flux derivative $\frac{\partial}{\partial z}(M_c u_c - u_E)$ for the a/ slow and b/ fast convective line. Line A indicates $\frac{\partial}{\partial z}(M_c u_E)$, line B indicates $\frac{\partial}{\partial z}(M_c u_c)$ for the case without horizontal pressure gradients, C indicates $\frac{\partial}{\partial z}(M_c u_c)$ with horizontal pressure gradient.

The comparison of the component of the vertical derivative of the momentum flux connected with the shear in the environmental wind $\frac{\partial}{\partial z}(M_c u_E)$, with the component describing the vertical change in the horizontal velocity in clouds $\frac{\partial}{\partial z}(M_c u_c)$, (Fig. 3-8) explains why this is the case. In the slow convective line vertical shear in the u - velocity is small and, when the horizontal pressure forces are taken into account, $\frac{\partial}{\partial z}(M_c u_c)$ has the magnitude comparable with $\frac{\partial}{\partial z}(M_c u_E)$. In the strong convective line, the changes in the cloud velocity caused by horizontal pressure gradients are larger than in the slow line but the shear in the direction parallel to the line is strong, and $\frac{\partial}{\partial z}(M_c u_E)$ term is dominant. It is worth noticing however, that although $\frac{\partial}{\partial z}(M_c u_E)$ is connected with the shear in the horizontal wind, since it is proportional to the first, not to the second derivative of u_E, it does not wipe out the maximum in the horizontal wind (as for example diffusion would do) but lowers its position.

3.2 Comparison with the GATE measurements

Some examples of the momentum fluxes measured in GATE fast and slow convective lines (LeMone et al., 1984) are shown in Fig. 3-9. Presented fluxes are normalized to 100 km-long flight legs. Since most of the momentum flux is created in the convective part of the line, we expect momentum flux in the first 30 km behind the leading edge to be significantly larger than that averaged over 100 km. Comparison of Figs. 3-4 and 3-6 with the momentum fluxes measured in GATE shows that momentum fluxes calculated in the parameterization are smaller than the 100 km averages from GATE. It is worth noticing however, that this underestimation of the momentum flux is similar for

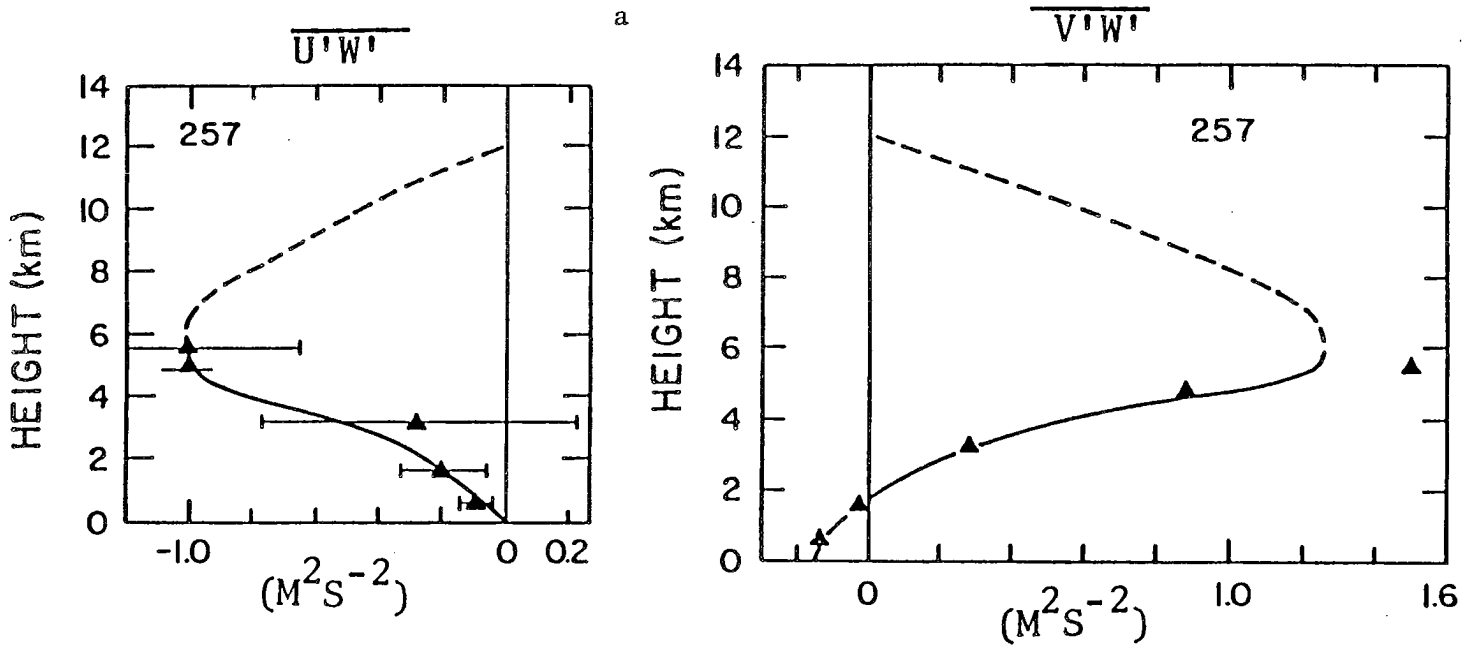

Fig. 3-9 Momentum fluxes for the a/ slow b/ fast convective lines as measured in GATE. The data are averaged over 100km - long flight legs.

b

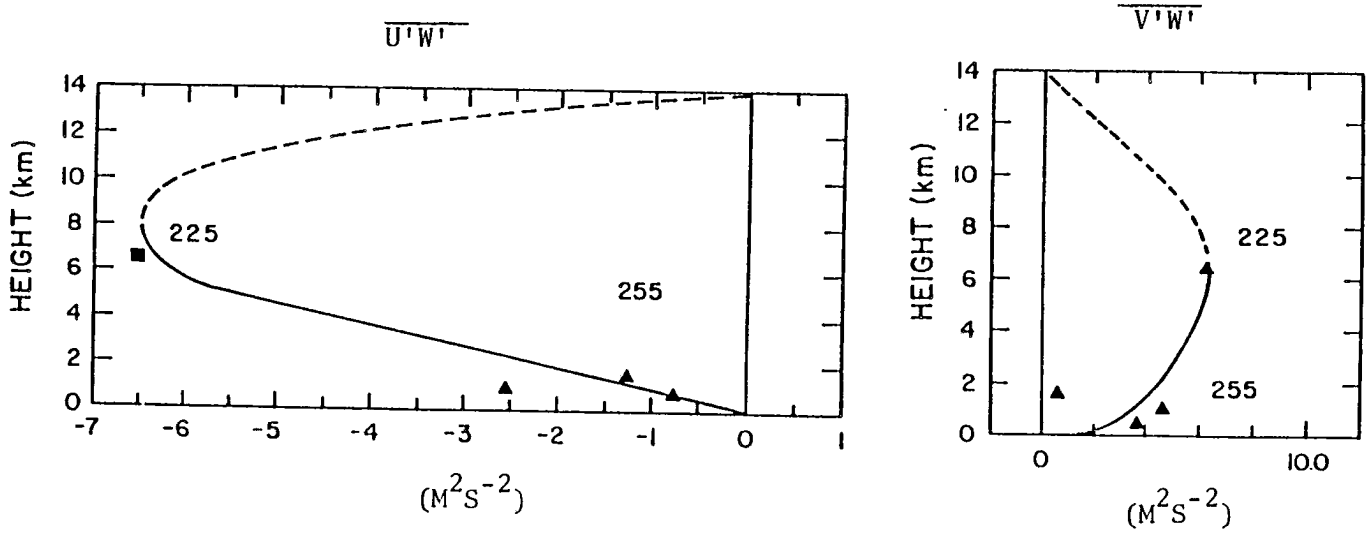

Fig. 3-9 (continued)

both line types and for both $\overline{u'w'}$ and $\overline{v'w'}$ momentum fluxes. According to the GATE measurements, the momentum flux in fast lines is about ten times larger that in slow lines. That fact agrees with our results (Fig. 3-4). Also, $\overline{v'w'}$ momentum fluxes are underestimated in the same degree as $\overline{u'w'}$. This suggests that it is the mass flux which is responsible for the underestimation of the momentum flux. Indeed, even when we use in calculation the observed vertical velocity in convective cores, the area occupied by the active convection calculated from the Fritsch and Chappell parameterization is still much smaller then area occupied by convective cores measured in GATE. Table 1a shows the fractional length of the GATE aircraft legs occupied by convective cores (Zipser and LeMone, 1980). Since roughly all convective cores occur in the convective part of the line, the fractional coverage by convective cores of the first 30 km behind the leading edge should appear as in Table 1b. The results shown in Table 1a are based on the measurements of different types of lines. To determine how our parameterization underestimates mass flux, we average the fractional coverage by updrafts for both types of lines (Fig. 3-3) and compare it with the values shown in Table 1b. It appears that the results of the parameterization are about 4.4 times smaller than the values measured in GATE. Since we use the vertical velocity in convective cores based on the GATE measurements, it suggests that our mass flux is also about 4.4 times too small. The reason for that may be the following.

The updraft mass flux on the cloud base in the Fritsch and Chappell parameterization is iterated until the available buoyant energy (APE) in the grid area is equal to zero. The reduction of APE

Altitude range (m)	Drafts		Cores	
	Up	Down	Up	Down
4300-8100	16.9	29.9	4.6	1.8
2500-4300	18.3	30.3	4.8	3.7
700-2500	16.3	25.2	2.1	1.1
300-700	16.6	18.8	1.5	0.8
0-300	15.9	15.7	0.3	0.2

Table 1a. Fractional length of aircraft legs occupied by drafts and cores (Zipser and LeMone 1980).

Altitude range (m)	Cores
	Up
4300-8100	15.3
2500-4300	15.3
700-2500	7.0
300-700	5.0
0-300	1.0

Table 1b. Fractional length of the convective region (30km) occupied by updraft cores (calculated from Table 1a).

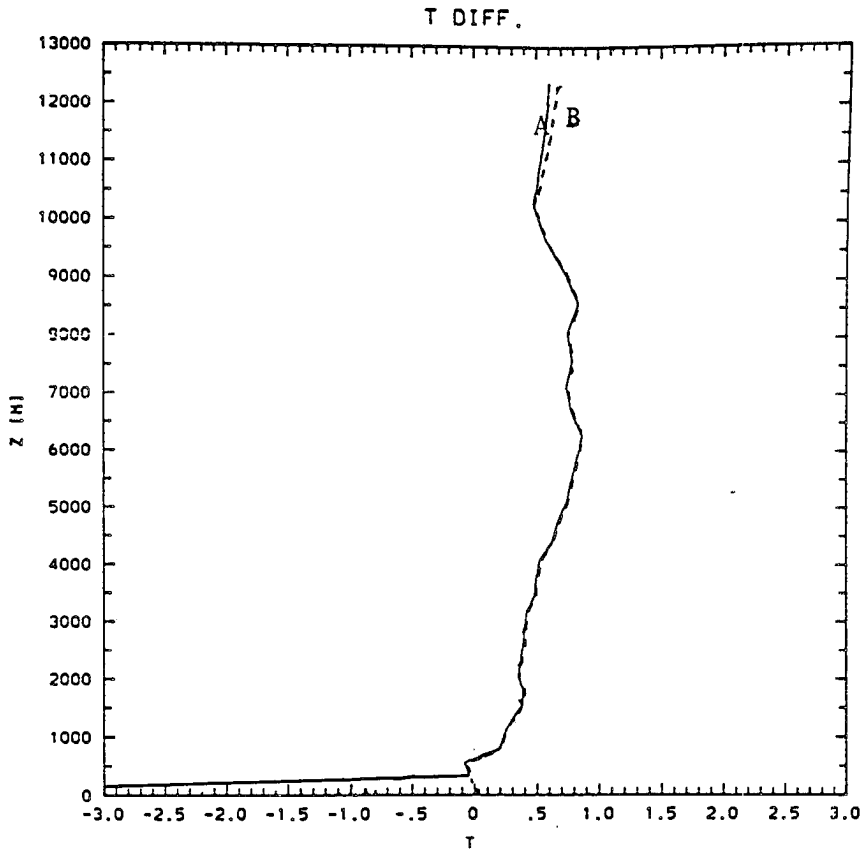

Fig. 3-10 Difference between the initial temperature of the environment and : A/ the temperature after parameterization averaged over the grid area, B/ the environmental temperature after the parameterization.

is achieved by the combination of the cooling of the layers close to the surface and the warming of the higher layers. The change in the grid area temperature depends mainly on the compensating subsidence. Only close to the ground does the spreading downdraft cause significant cooling of the lowest layer (Fig. 3-10). This means that the cloud mass flux calculated in the Fritsch and Chappell parameterization depends mainly on parameters influencing the compensating subsidence. The compensating subsidence depends on two factors: cloud mass flux and the mean vertical velocity in the grid area. We will show how the change in the magnitude and the vertical structure of these parameters influences the heating of the environment and, as a result, the magnitude of the cloud mass flux needed to reduce the available buoyant energy to zero.

Following Fritsch and Chappell (1980) the compensating subsidence is calculated from:

$$w_E = (A\bar{w}\bar{\rho} - A_u w_u \rho_u - A_D w_D \rho_D)(A_E \rho_E)^{-1} \qquad (4.1)$$

It can be seen from the above equation that if the mesoscale vertical velocity $\bar{w}$ is larger than zero, the same updraft mass flux causes smaller compensating subsidence than that which occurs in the case with zero mean vertical velocity. This means that the increase in the mean vertical velocity will increase the cloud mass flux needed to reduce APE. In addition, when the mean vertical velocity increases with height, heating of the higher layers is smaller and the updraft mass flux needed to reduce the APE has to be even larger than in the former case. This example is illustrated in Fig. 3-11.

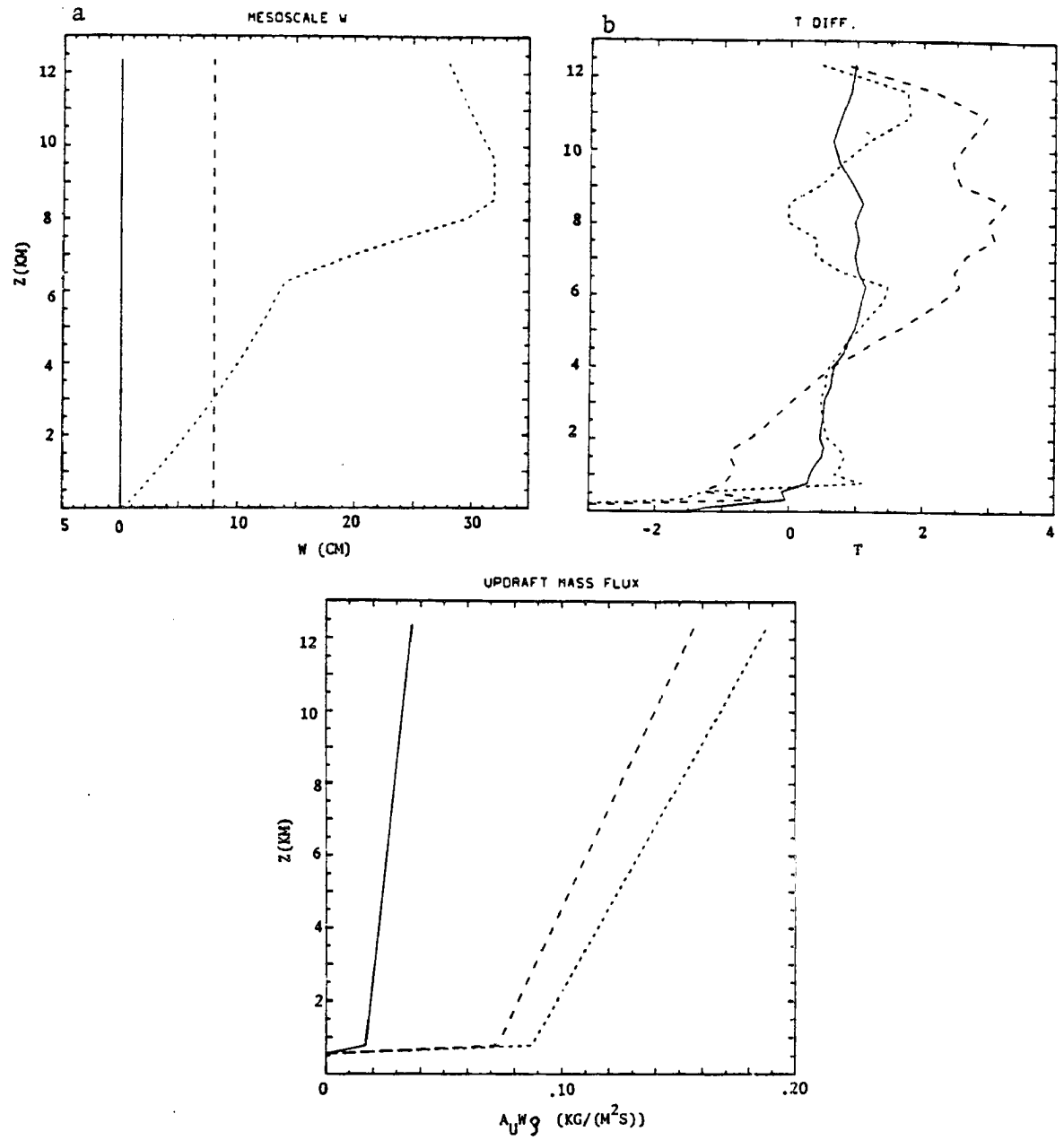

Fig. 3-11 Sensitivity of the calculated mass flux to the change in the mesoscale mean velocity. a/ mesoscale $\bar{w}$ used in the test, b/ change in the grid box temperature obtained for different w from the 3-11a, c/ mass fluxes calculated with the different w from 3-11a.

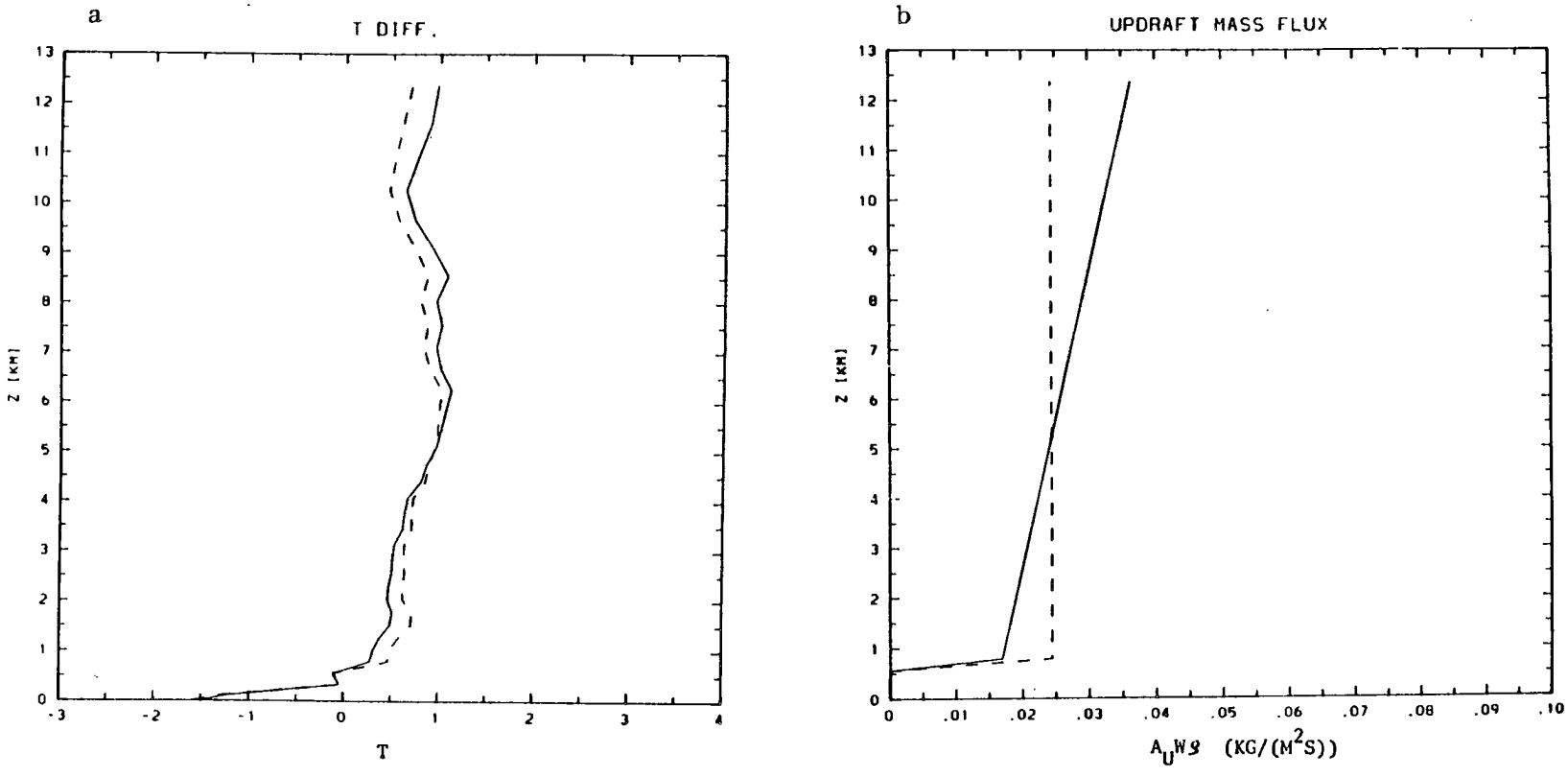

Fig. 3-12 Sensitivity of the calculated mass flux to the lateral detrainment; a/ change in the grid box temperature, b/ calculated mass flux. The solid lines indicate the case with entrainment rate equal to detrainment rate (mass flux constant with height), the dashed lines indicate the case with zero lateral detrainment.

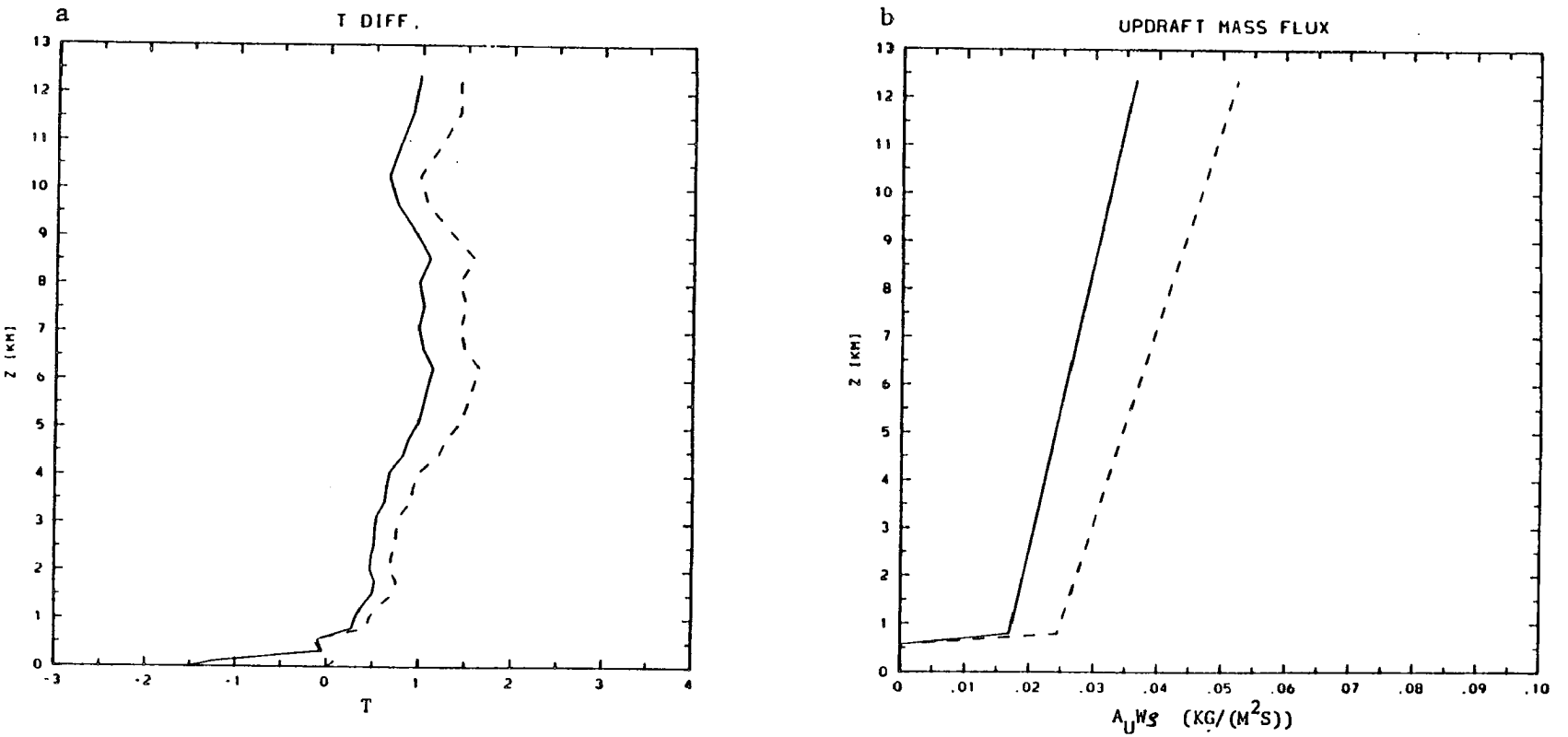

Fig. 3-13 Sensitivity of the calculated mass blux to the low-level heating; a/ change in temperature, b/ mass flux. Solid lines indicate the case when low level air was cooled by spreading downdraft; dashed lines indicate the case when cooling by downdraft was neglected.

On the other hand, when updraft mass flux is increasing with height (for example with no lateral detrainment), warming of the higher levels is stronger than in the case of the updraft mass flux constant with height (entrainment=detrainment). This implies that the mass flux needed to reduce APE to zero has to be larger in the case of updraft mass flux constant with height. This is illustrated in Fig. 3-12.

Even though heating caused by compensating subsidence dominates, stronger cooling of the lower layers by downdraft air can also help to reduce APE and, consequently, to reduce updraft mass flux calculated in the parameterization. Fig. 3-13 shows the increase of the mass flux caused by neglecting the cooling of the lowest layer by the spreading downdraft air.

It can be seen from the above analysis that the mean mesoscale vertical velocity is a very important factor in the calculations of the convective heating and the cloud mass flux. Fig. 3-14 shows that the vertical velocity in the slow convective line averaged over the first 30 km behind the leading edge can be even larger than that used in the sensitivity test presented above. Because of the lack of data above the 6 km level, we did not try to reproduce the convective heating and mass flux using the mesoscale vertical velocity from Fig. 3-14, but we believe that non-realistic w is the source of our underestimation of the cloud mass flux and momentum flux. Fig. 3-15 shows the comparison of the momentum flux for the slow line calculated with the correction to the realistic mass flux, with the momentum flux measured in the slow line observed during GATE on 14 September 1974 (LeMone, 1983). The data for the 14 September line are averaged over

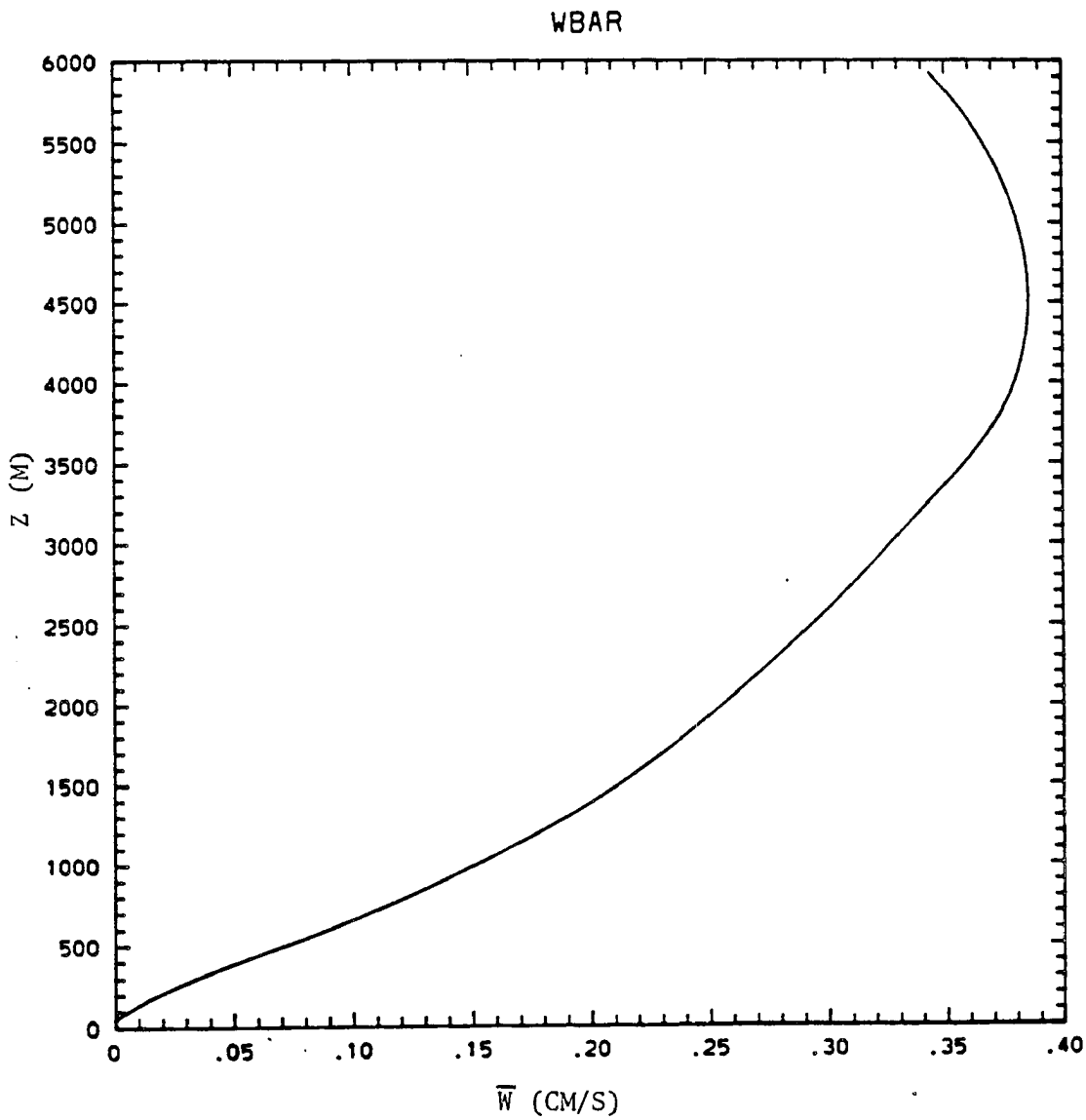

Fig. 3-14 Vertical velocity in the 14 September convective line (LeMone, 1983) averaged over first 30km behind the leading edge.

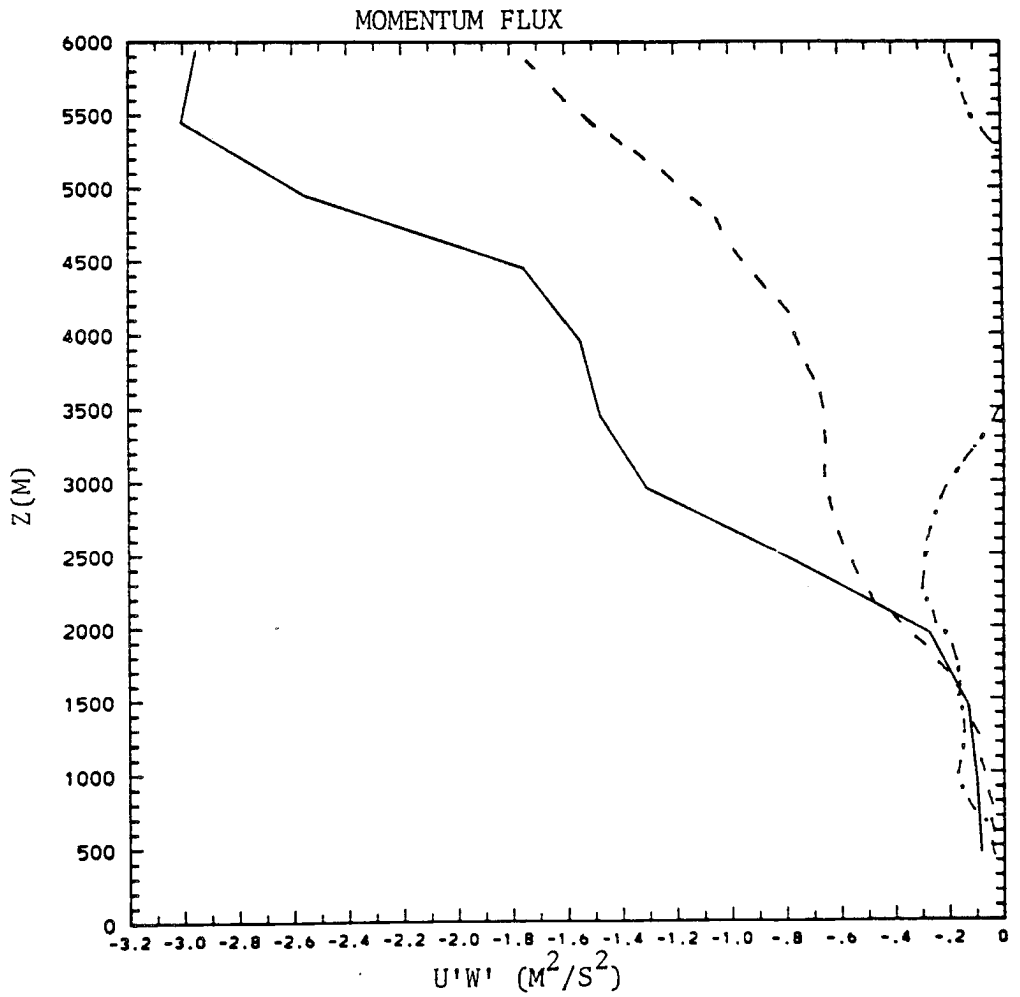

Fig. 3-15 Comparison of the $\overline{u'w'}$ momentum flux from the 14 September convective line (LeMone, 1983), averaged over first 30km behind the leading edge (solid line) with the momentum flux calculated in the parameterization and corrected for observed mass flux with (dashed line) and without (dot-dashed line) horizontal pressure gradients.

the first 30 km behind the leading edge. It can be seen that the pressure forces play a dominant role in creating the momentum flux which resembles that measured in GATE. Calculated momentum flux, even after corrections for pressure forces and realistic mass flux, is still smaller than the momentum flux of the 14 September line, but this can be caused by the fact that we compare momentum flux calculated for the composite slow line with the momentum flux for a particular case.

3.3 Implications for the mesoscale numerical models

The problem with estimating the mean mesoscale vertical velocity is avoided when parameterization is used in numerical model, where w is supplied by the model itself. The other factors (lateral detrainment, low-level cooling) do not drastically change the mass flux calculated in the parameterization, so we believe that the parameterization used in the numerical model which predicts realistic $\bar{w}$ should produce reasonable magnitudes of mass and momentum fluxes. It is then worthwhile to see what the influence of the subgrid pressure gradients on the mean mesoscale wind can be, compared with other terms in the mesoscale momentum equation. To do so, we use the momentum fluxes calculated in Fritsch and Chappell parameterization and corrected for the observed mass flux. We also use two-dimensional wind fields for the line from LeMone (1983) paper. Fig. 3-16 shows the profiles of the different terms in the u-momentum equation, averaged over 30 km. The correction for the horizontal pressure gradients is calculated as the difference between vertical derivatives of the momentum flux with and without pressure gradients. It can be

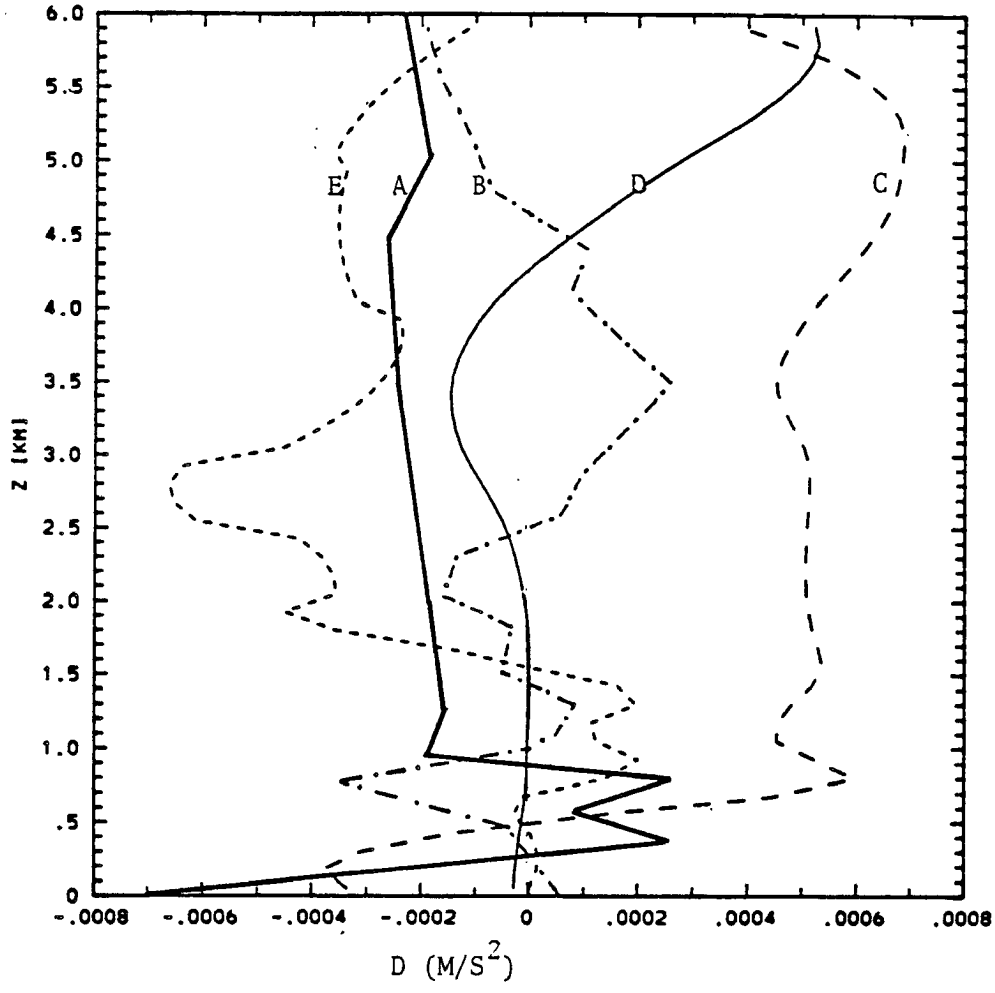

Fig. 3-16 Comparison of the change in the vertical derivative of the momentum flux generated by convection with other terms in the mesoscale u-momentum equation. A - horizontal pressure gradient effect on momentum flux derivative, B - vertical derivative of the momentum flux calculated without horizontal pressure gradients, C - horizontal pressure gradient averaged over 30km, D - horizontal advection, E - vertical advection.

seen that the effect of the horizontal pressure gradient has a magnitude comparable with the other terms in the momentum equation. It seems that at least in the slow-moving convective line that effect must be taken into account.

3.4 Summary

1. The vertical flux of the horizontal momentum in the Fritsch and Chappell parameterization is generated mainly by updrafts. The effect of downdrafts on the total momentum can be neglected. The parameterization estimates properly the difference between momentum flux in the fast and slow lines, but the magnitude of the momentum flux is underestimated.

2. The magnitude of the momentum flux calculated in Frisch and Chappell parameterization strongly depends on the mesoscale vertical velocity used in the calculations of the convective mass flux. When, as assumed in our calculations, the mesoscale vertical velocity is equal to zero (with the compensating subsidence occuring in the area 4 times bigger then the grid area), the convective mass flux and momentum flux is underestimated by a factor of 4.4. This problem however, seems to be easy to avoid in numerical models where mesoscale velocity is provided by the model.

3. The influence of the pressure forces on momentum flux strongly depends on vertical velocities in convective drafts. Realistic vertical velocities are needed to evaluate the effects of horizontal pressure gradients.

4. Taking pressure forces into account brings values of momentum flux much closer to those measured in GATE. In the case of the slow

convective line, neglecting the horizontal pressure gradients changes not only the magnitude, but also the sign of the momentum flux. For the fast convective line, including horizontal pressure forces changes the magnitude of the momentum flux, but effects connected with the strong environmental wind shear are dominant.

5. Calculations for the slow convective line show that when the realistic vertical velocities in convective drafts and the realistic cloud mass flux are used, the effect of the horizontal pressure gradient (the difference between vertical derivative with and without pressure terms) has a magnitude comparable with the magnitude of the mesoscale (averaged over 30 km) terms in the momentum equation. We conclude that in modeling of the slow convective lines, cloud-scale pressure forces should be taken into account in parameterization of the subgrid momentum flux.

IV. Lagrangian Calculation for the Movement of the Parcel in the Pressure Field Generated in the Convective Line

In the previous chapters we discussed the parameterization of the momentum flux generated in the convective line, using a 1D cloud model and composite soundings for the environment of the fast and slow convective line. In our calculations we did not take into account the fact that convective cores move in the environment changed already by convection, except in the momentum equation, where we used convection-generated horizontal pressure gradients. We also had to use the vertical velocity in updraft and downdraft taken from measurements, rather than calculated in parameterization, in order to obtain the realistic momentum flux. In this section we would like to evaluate the effect of the horizontal pressure gradients on the momentum flux in the convective line using a somewhat different approach. Instead of looking at one cloud type and the 1D cloud model, we consider the movement of the set of Lagrangian parcels ("convective cores"), with different initial conditions, moving in the two-dimensional pressure field. We will also take into account vertical gradients of the convection-generated pressure disturbance which were neglected in calculations done in the previous chapter.

4.1 Description of the calculations

The Lagrangian parcel accelerates under the influence of gravity, vertical pressure gradient force, and liquid water drag in the

vertical direction and horizontal pressure gradient force in the horizontal direction. When we use the coordinate system moving with the line with the axes directed as in the previous chapter the quations of motion have the form:

$$\frac{Du}{Dt} = -\frac{1}{\rho}\frac{\partial p_D}{\partial x} + \varepsilon u_E \tag{4.1}$$

$$\frac{Dw}{Dt} = -\left(\frac{1}{\rho}\frac{\partial p_D}{\partial z} + \frac{T_p - T_s}{T} - gq_L\right)/(1+\alpha) + \varepsilon w_E \tag{4.2}$$

where u is the horizontal velocity in the x direction, w is the vertical velocity and p_D is the pressure disturbance generated by convection. They buoyancy term in the equation 4.2 is calculated relative to the environmental composite sounding shown in Fig. 22a. T_p is the parcel virtual temperature, T_s is the virtual temperature on the level z given by the composite sounding. The term gq_L describes a liquid water drag, where q_L is the liquid water content calculated with the assumption that rain efficiency is equal to 0.5 and q_{Lmax} is equal to 4g/kg. As in the previous chapter (see also Appendix B), we take into account the virtual mass effect ($\alpha = .5$ is the virtual mass coefficient). Mixing with the environment is considered in the same way as in the Fritsch and Chappell parameterization (ε is an entrainment coefficient), with the assumption that the cloud top is at 12 km. The parcel is moving dry adiabatically below the lifting condensation level (LCL) and moist-adiabatically above LCL. We use the same data as in the previous chapters; this means composite sounding for the slow line shown in Fig. 2-2a and pressure disturbances field shown in Fig. 2-3a. We also use the disturbances of the virtual temperature calculated from the pressure disturbances

(Fig. 2-4) to determine the temperature of the air mixed into the parcel. The initial temperature for every parcel is assumed to be equal to the environmental temperature (temperature from the sounding plus the correction calculated from the pressure disturbances). As in the Fritsch and Chappell parameterization, the initial vertical velocity in every case is equal to 1 m/s.

4.2 Results

We consider Lagrangian parcels moving in the pressure disturbance field for the slow convective line, originating in points (x_o, z_o) where: z_o = 100, 200, 300, 400, 500 m and x_o = -300, -4300, -8300, -12300, and -16300 m. Figs. 4-1 to 4-3 show the vertical and horizontal forces acting on the parcel depending on the initial position of the parcel in the convective line. The resulting trajectories, velocities and momentum fluxes are plotted in Figs. 4-4 to 4-6. The parcels which originate in the lower layer (100-300 m) and close to the leading edge (Fig. 4-1) have the highest initial temperature and are the most buoyant. They can reach large vertical velocities of the order 14 m/s (Fig. 4-4a). Parcels originating in the lower layer, but farther from the leading edge (Fig. 4-2) have a lower initial temperature and smaller buoyancy, but below 1500 m they are accelerated abruptly by a strong vertical pressure gradient force (Fig. 4-2b). The resulting vertical velocity is large below 1500 m, but it increases slowly above 1500 m, and finally it reaches values smaller than those for parcels starting close to the leading edge (Fig. 4-4b). The parcels originating on the higher level (400-500 m) have the smallest buoyancy (Fig. 4-3a). They move through the line

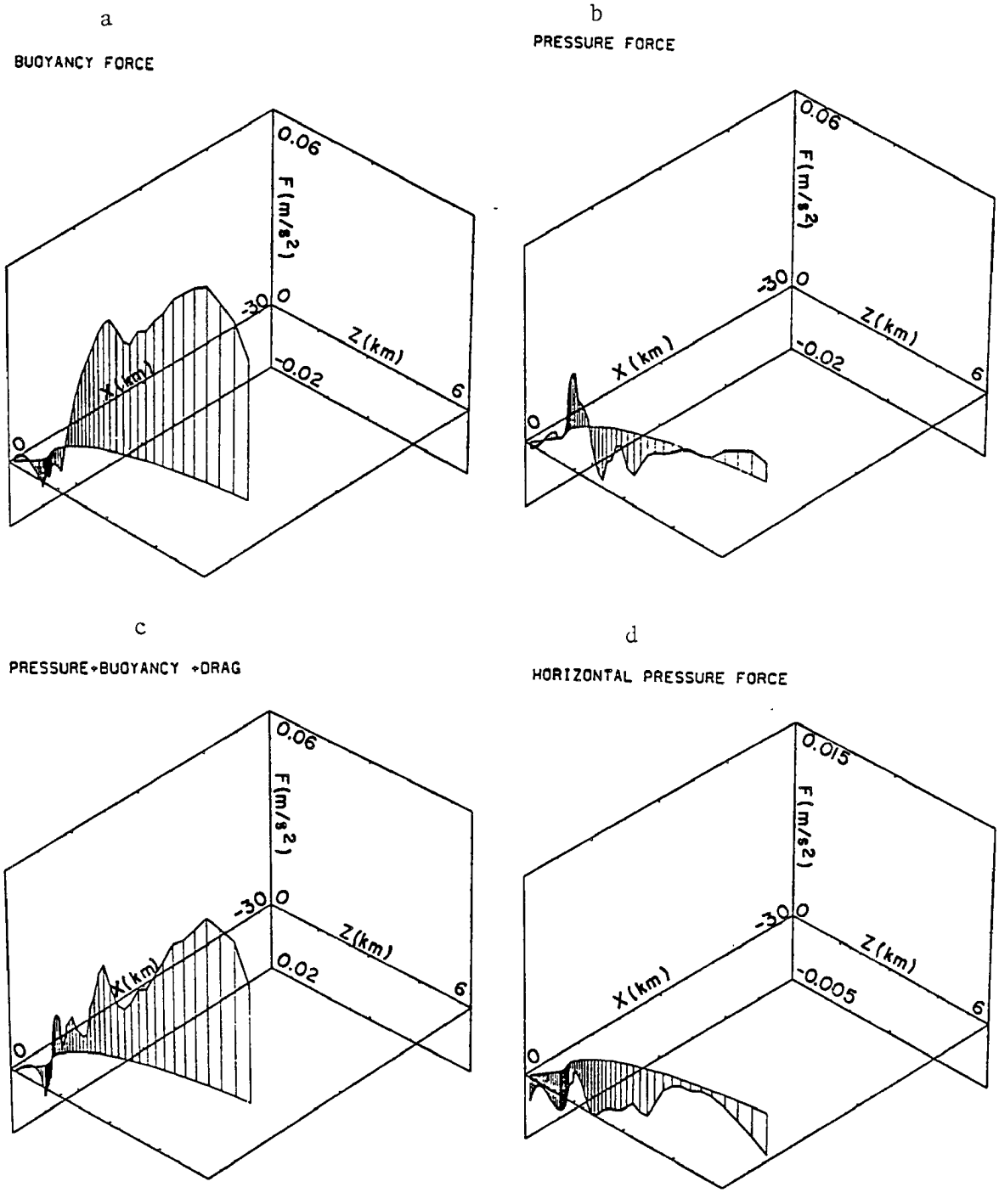

Fig. 4-1 Forces acting on the parcel which originate in the point x_0 = -300m, z_0 = 100m. a/ buoyancy, b/ vertical pressure gradient, c/ buoyancy + vertical pressure gradient + liquid water drag, d/ horizontal pressure gradient. Note: In Figs. 4-1 to 4-3 fine vertical lines ("fence") indicate time steps.

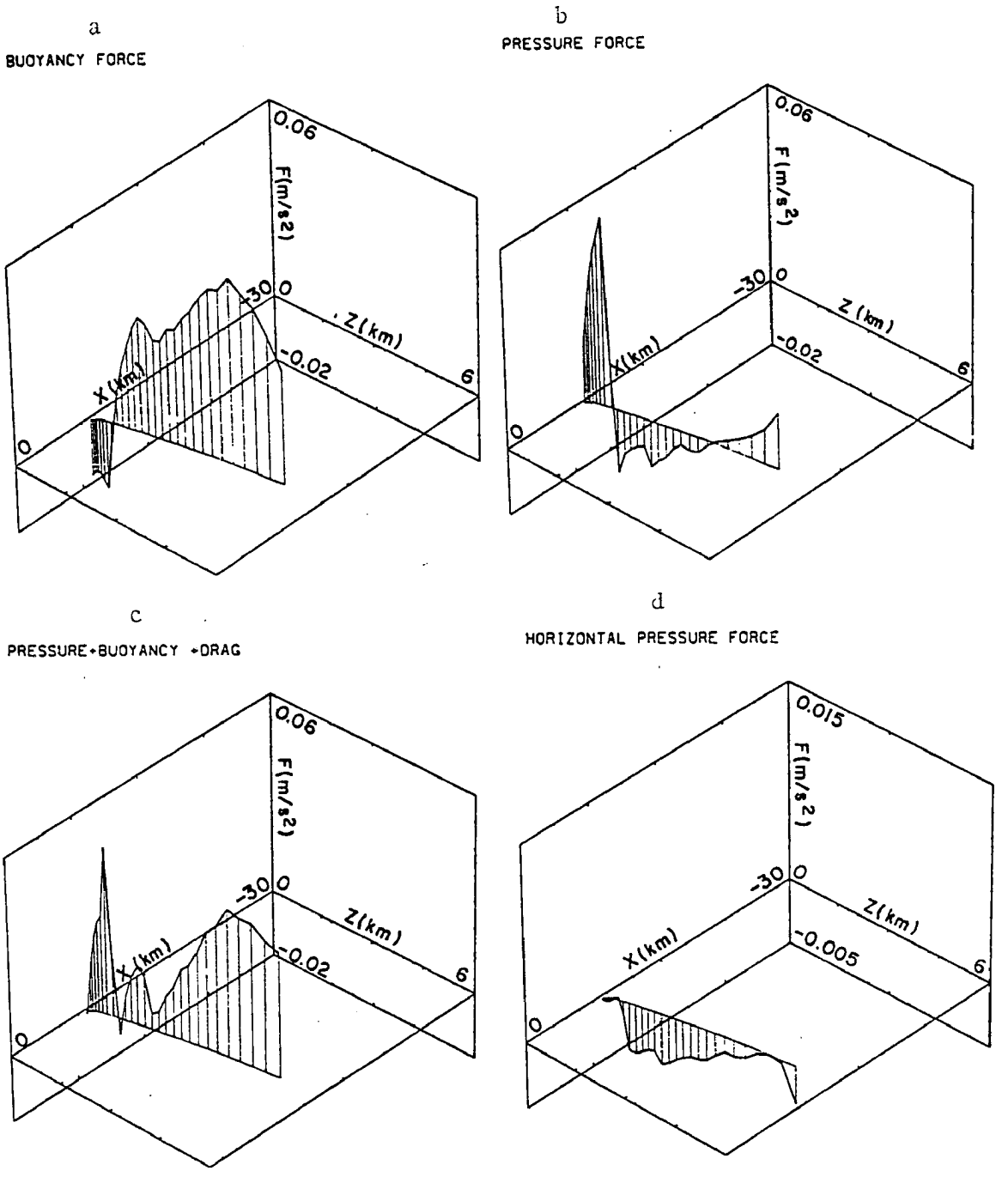

Fig. 4-2 Forces acting on the parcel which originate in the point x_0 = -8300m, z_0 = 100m. a/ buoyancy, b/ vertical pressure gradient, c/ buoyancy + vertical pressure gradient + liquid water drag, d/ horizontal pressure gradient.

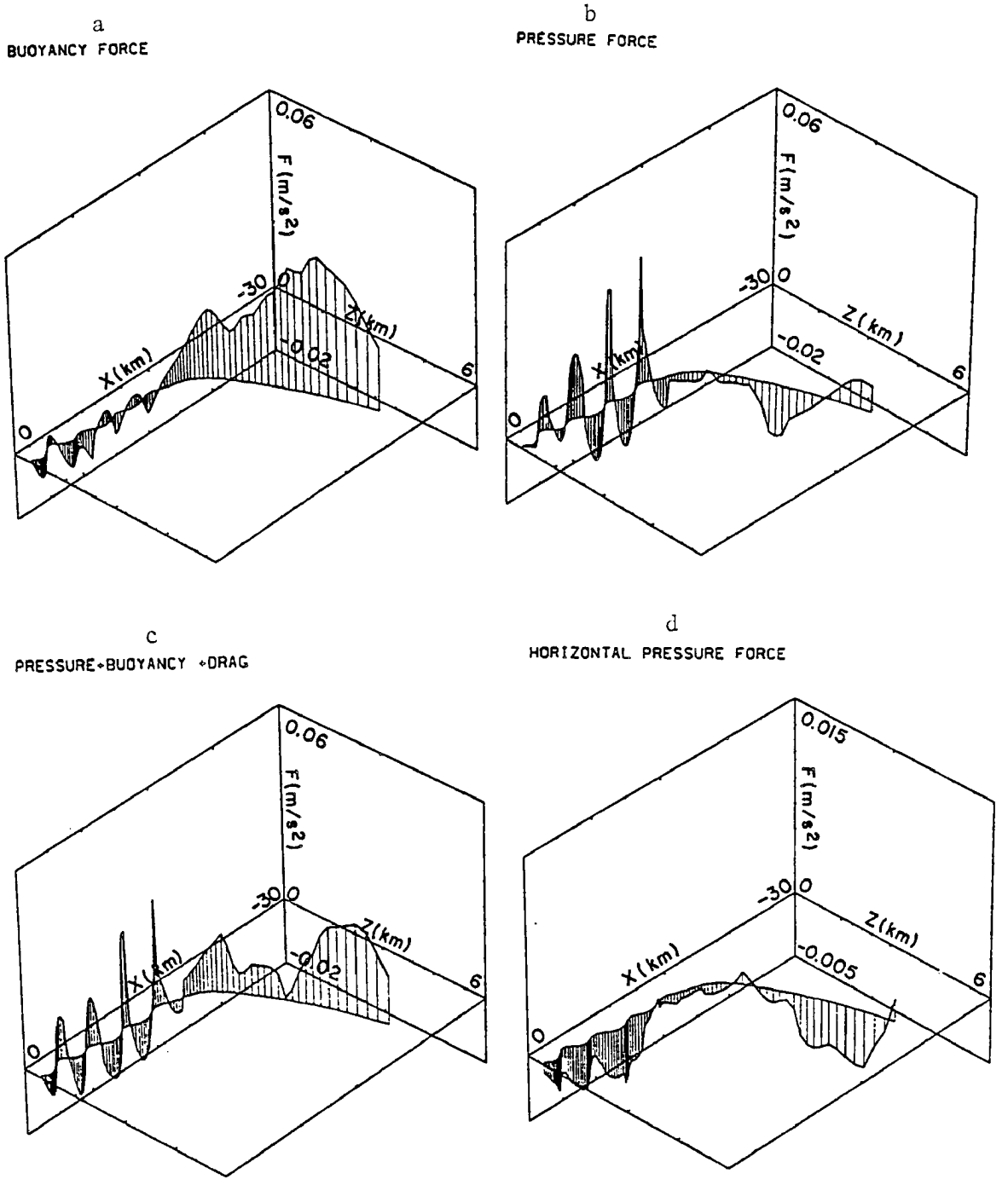

Fig. 4-3 Forces acting on the parcel which originate in the point x_0 = -300m, z_0 = 500m. a/ buoyancy, b/ vertical pressure gradient, c/ buoyancy + vertical pressure gradient + liquid water drag, d/ horizontal pressure gradient.

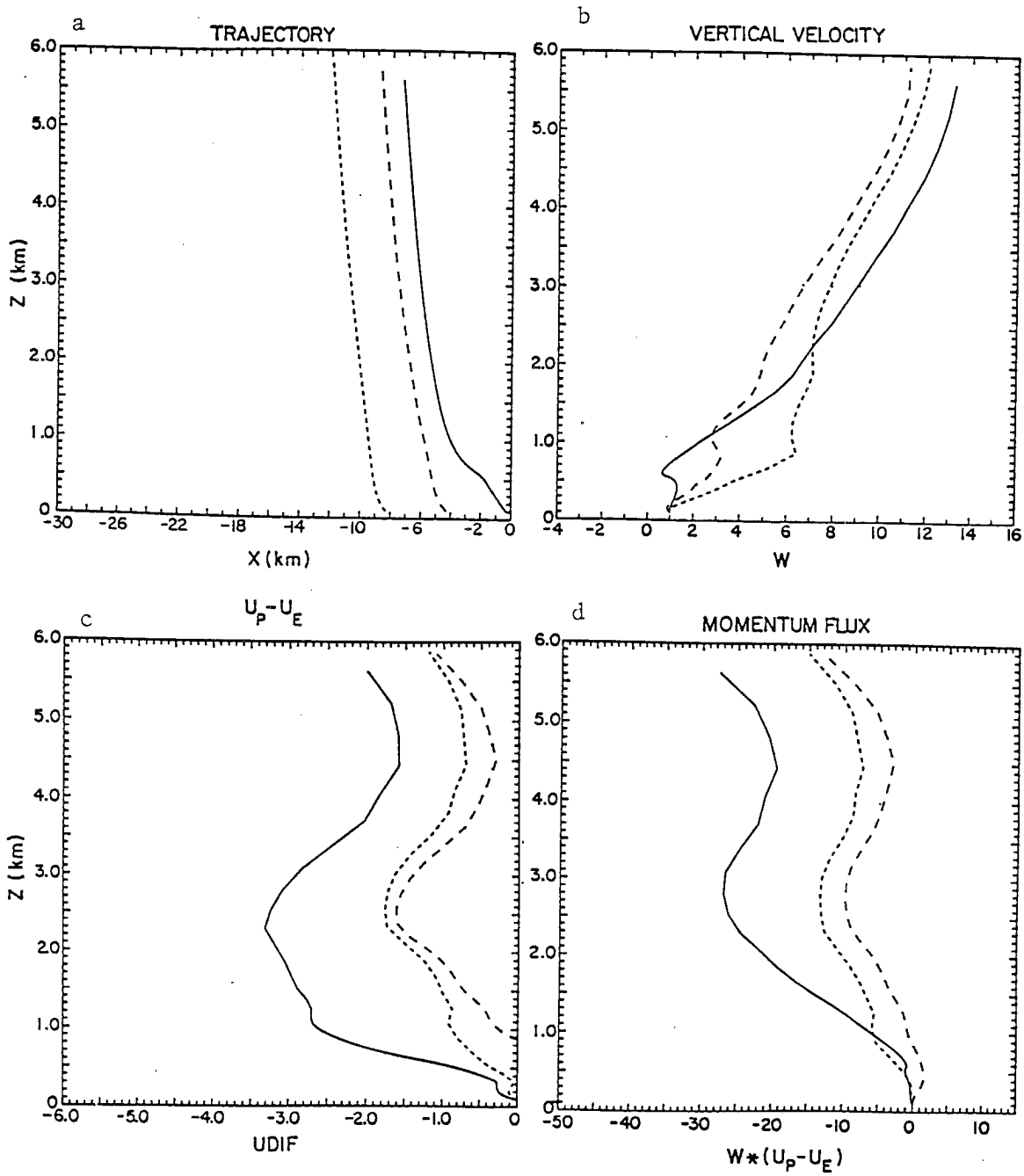

Fig. 4-4 Examples of the trajectories, vertical velocities, momentum ($u_p - u_E$) and momentum fluxes for the parcels originating on z_{0_p} = 100m. Solid lines indicate x_0 = -300m, dashed lines x_0 = -4300m, fine dashed lines x_0 = 8300m.

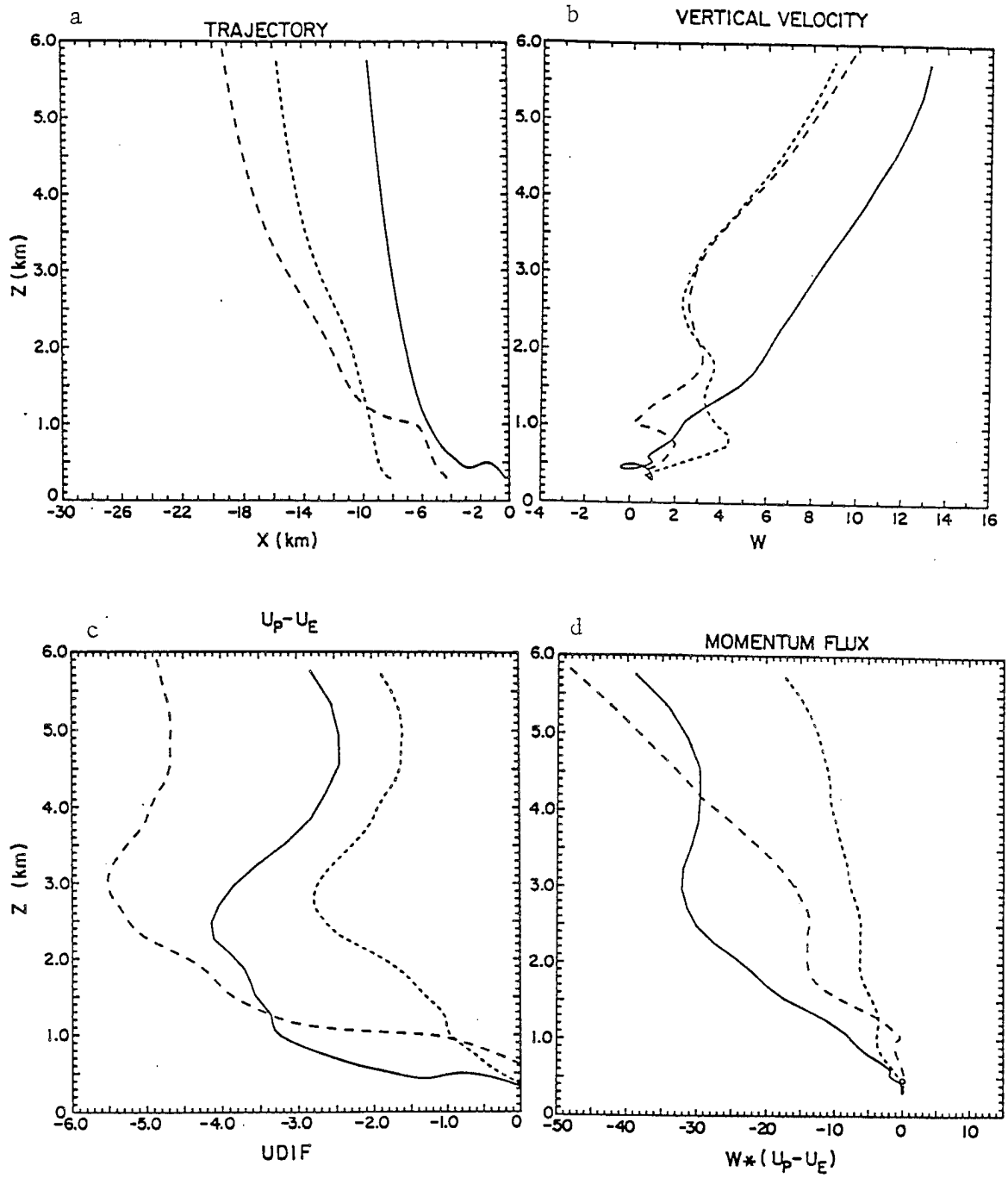

Fig. 4-5 Examples of the trajectories, vertical velocities, momentum ($u_p - u_E$) and momentum fluxes for the parcels originating on z_0 = 300m. Solid lines indicate x_0 = -300m dashed lines $-x_0$ = -4300m, fine dashed lines x_0 = -8300m.

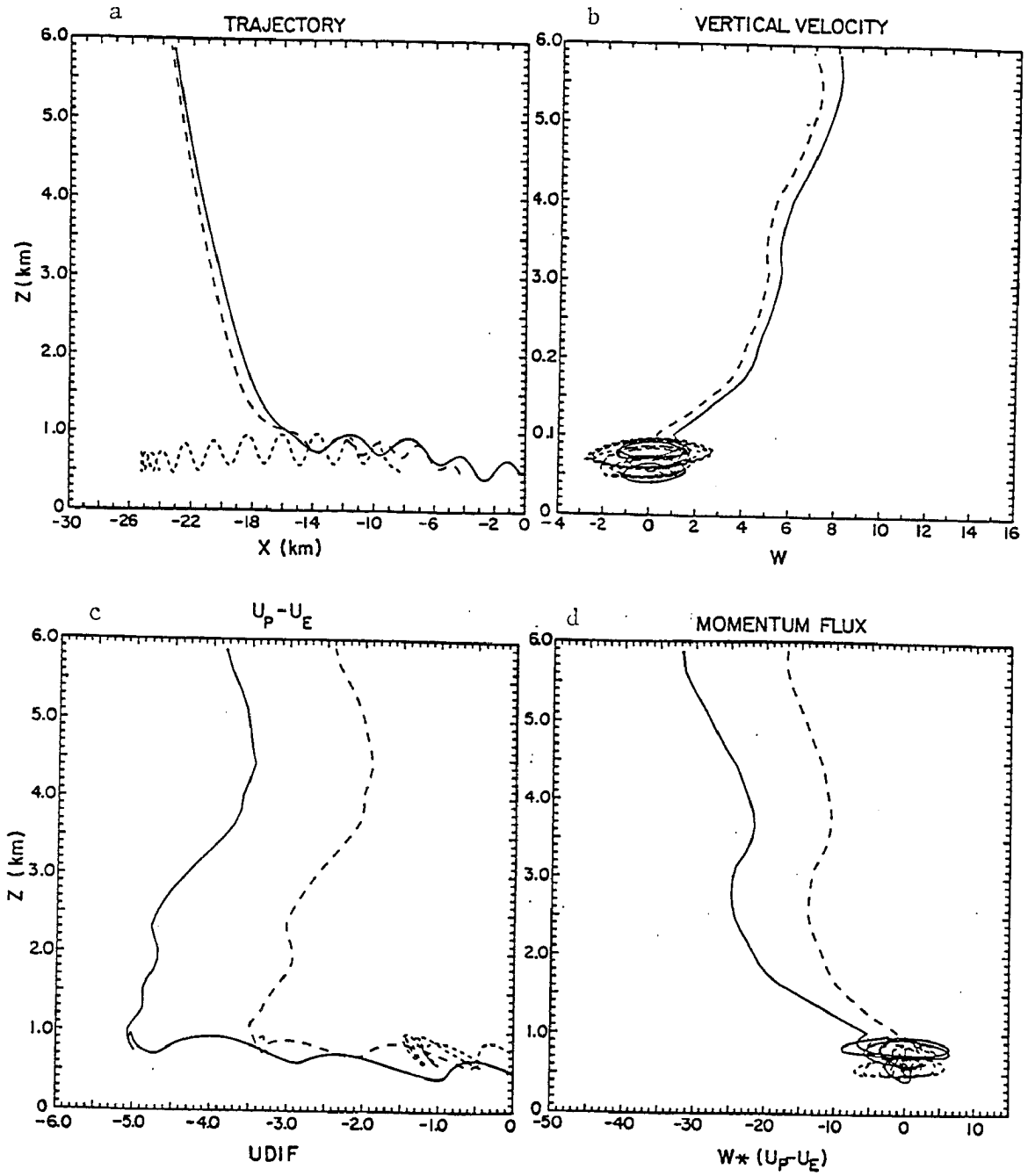

Fig. 4-6 Examples of the trajectories, vertical velocities, momentum, and momentum fluxes for the parcels originating at z_0 = 500m. Solid lines indicate x_0 = 300m, dashed lines $-x_0$ = -4300m, fine dashed lines x_0 = -8300m.

until they are pushed up by the strong vertical pressure gradient close to the low center (Fig. 4-3b). They have the smallest vertical velocities and, as seen in Fig. 4-6a, the parcels starting at this level and closer to the low center do not have enough buoyancy to form an updraft.

The change of parcel momentum caused by horizontal pressure gradients depends on the vertical velocity profile for the parcel and, as a consequence, on the initial position of the parcel. For example, as can be seen in Fig. 4-3c, the parcel originating at 500 m stays for a long time in the region with the large horizontal pressure gradient and gains the high momentum (Fig. 4-6c). Parcels starting at the lower levels spend less time under the influence of the large horizontal pressure gradient. The change of their momentum is usually smaller and depends on the distance of the initial position of the parcel from the low center. Parcel starting close to the low center ($x_o < -8300$) gain less momentum than the parcels originating in the vicinity of the leading edge (Fig. 4-1c and 4-2c). The examples of the trajectories, vertical velocities, horizontal momentum ($u_p - u_E$), and the vertical flux of horizontal momentum ($w(u_p - u_E)$) for different parcels are shown in Figs. 4-4 to 4-6.

To determine how the properties of the Lagrangian parcels in our calculations compare to the properties of the convective cores measured in GATE, we calculate mean vertical velocity and mean vertical momentum flux for our "cores". As in the GATE measurements, we assume that the parcel represents a convective core if it has a vertical velocity larger then 1 m/s. Fig. 4-7 shows that up to 3 km, the mean vertical velocity of the Lagrangian parcels is roughly equal

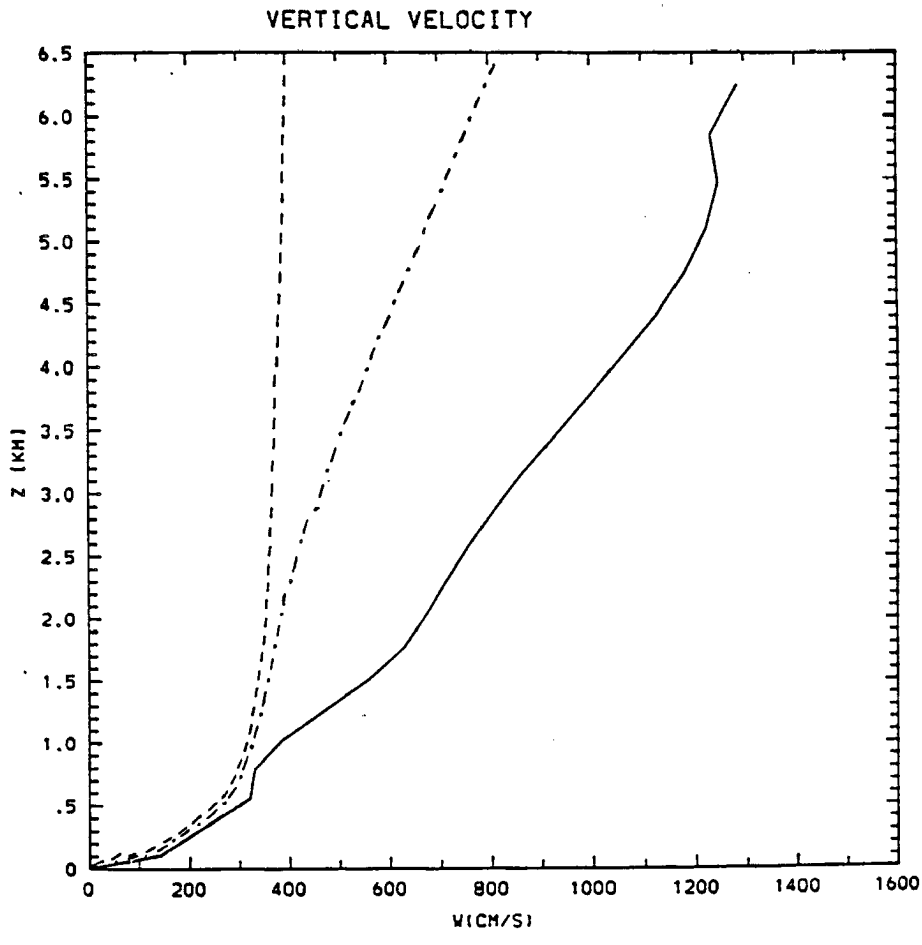

Fig. 4-7 Comparison of the calculated and measured vertical velocity in the convective cores. Dashed line - median w_{max} in GATE convective cores, solid line - vertical velocity in the updraft as calculated in Fritsch and Chappel parameterization in Chapter III, dotdashed line - average vertical velocity for the set of Lagrangian parcels.

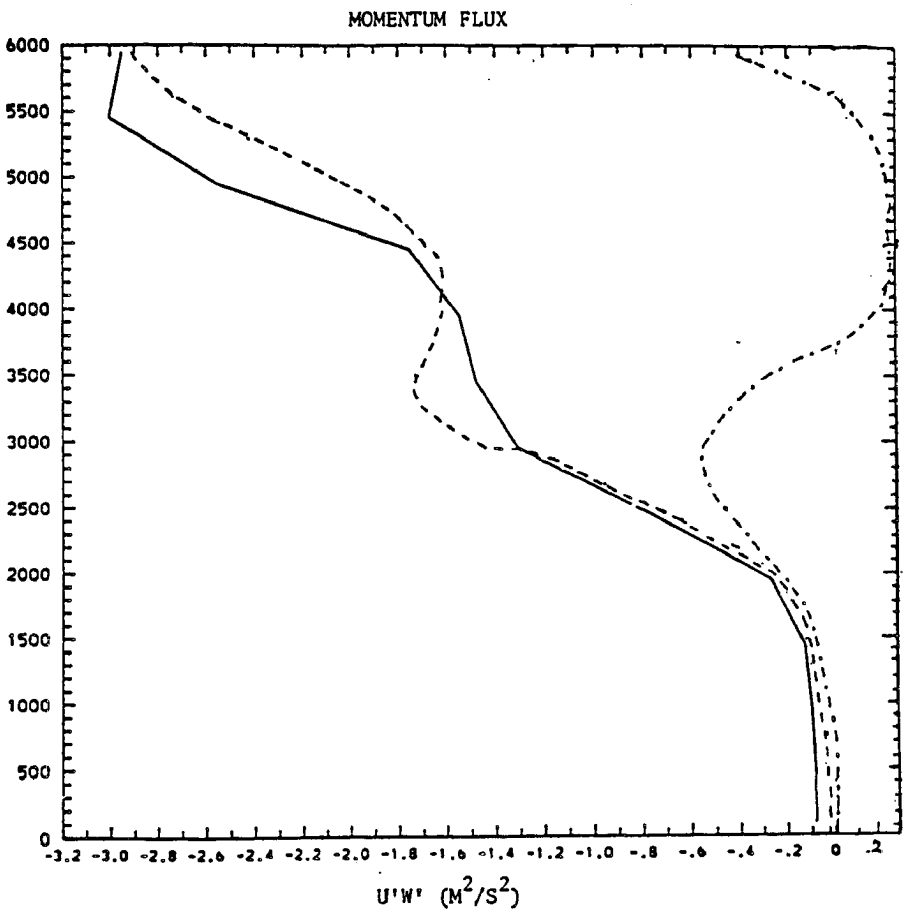

Fig. 4-8 Comparison of the measured and calculated vertical flux of the horizontal momentum. Solid line - momentum flux for the 14 September convective line averaged over the first 30km behind the leading edge, dashed line - average momentum flux for Lagrangian parcels calculated with the horizontal pressure gradients, dot-dashed line - average momentum flux for the Lagrangian parcels calculated without pressure gradients.

to the median maximal vertical velocity w_{max} in the GATE convective cores (for definition of w_{max} see LeMone and Zipser (1980)). At the higher levels (above 3 km) the average vertical velocity for Lagrangian parcels is larger than the median GATE core velocities, but it is significantly closer to the observed w than the vertical velocity in updraft calculated in the Fritsch and Chappell parameterization.

Fig. 4-8 shows the effect of horizontal pressure gradients on the momentum flux of the Lagrangian parcels. Momentum fluxes for all the parcels calculated as $w(u_p - u_E)$ are averaged and multiplied by the fractional coverage by the cores in the convective part of the line (Table 1b). This procedure is used for the cases with and without horizontal pressure gradients. As in the previous chapter, both momentum fluxes are compared with the momentum flux for the 14 September slow convective line, averaged over the first 30 km behind the leading edge. The results agree with those obtained in the Fritsch and Chappell parameterization for the slow convective line corrected for the realistic vertical velocities and mass flux, although magnitudes of momentum fluxes differ by the factor of two (this difference can be caused by the fact that fractional coverages by convective cores shown in Table 1b, describe measurements for the different types of lines). In the absence of horizontal pressure gradients, momentum flux is small and changes the sign depending on the enviromental wind shear. When the horizontal pressure gradients are taken into account, momentum flux below 6 km is negative and has a magnitude close to that measured in GATE.

4.3 Summary

1. The use of the 2D convection-generated pressure field, and of the set of Lagrangian parcels moving in this field with different initial conditions, allows us to obtain the mean vertical velocity in cloud which agrees better with measurements than that obtained in the Fritsch and Chappell parameterization.

2. The results of the calculations presented above support the conclusions obtained in the previous chapter, i.e., that in the 2D convective line, the horizontal pressure forces play an important role in the generation of the momentum flux. The mean momentum flux for the convective parcels looks like the measured momentum flux for the slow convective line, only if horizontal pressure gradients are included in the calculations.

V. Concluding Discussion

The main purpose of this study is to evaluate the influence of the subgrid horizontal pressure gradients on convective momentum fluxes in two-dimensional tropical convective lines. In addressing this problem we have used two techniques and both of them gave similar answers. In 2D convective lines, especially the slow moving lines, the horizontal pressure forces play a crucial role in creating momentum fluxes corresponding to those observed in GATE. We have shown that for the slow moving line, it is not possible to obtain either the observed magnitude or the sign of momentum flux, unless the horizontal pressure gradient effects are included. We also looked at the different terms in the u momentum equation averaged over 30 km, and concluded that the change of the vertical derivative of the subgrid momentum flux caused by subgrid scale horizontal pressure gradient has magnitude comparable with the other terms in the momentum equation. This result suggests that in modeling of the convective (particularly slow-moving) lines, horizontal pressure gradients should be taken into account. However, although both our techniques appeared to be useful in answering the question of how important horizontal pressure forces are in creating observed momentum flux, neither of them can be used in a numerical model to actually calculate momentum fluxes. Calculations for the Lagrangian set of parcels used GATE data extensively and were just a method of looking at the existing data

set. The Fritsch and Chappell parameterization allowed us to calculate mass and momentum fluexes, but it had at least two deficiencies. The mass and momentum fluxes were underestimated and vertical velocities in convective drafts were too large compared to those observed in GATE. We showed that underestimation of the mass and consequently momentum flux was probably caused by nonrealistic mean mesoscale velocity used in our calculations and can be avoided in a numerical model. The overprediction of the vertical velocity in convective drafts is, however, a more serious problem because it causes the underestimation of the horizontal pressure gradient influence on momentum. The results of Lagrangian calculations give us some suggestions on how the calculations of the vertical velocity in clouds (and as a result momentum flux) can be improved. In the Fritsch and Chappell parameterization the updraft velocity was represented by the velocity of the parcel with the average characteristics of the most buoyant layer. Our calculations for the set of Lagrangian parcels in 2D pressure field showed that when the vertical pressure gradients were taken into account and the set of parcels with different initial temperatures were considered, the average vertical velocity was much closer to the observed one. In the Lagrangian calculation we used the coordinate system moving with the line, so we believe the parcels originating at different distances from the leading edge represent the updraft at the given point in different stages of cloud development. Therefore, we think that convective parameterization attempting to account properly for the horizontal pressure gradient effects hould have the following features. The first is a time dependent cloud model and time dependent coupling

between cloud scale and mesoscale. This would allow to take into acount the change in the convective environment and the change in properties of updraft and downdraft. The second improvement which could be made is considering not only the horizontal but also vertical pressure gradient forces. The importance of this introduction was already shown by Holton (1973). Such a parameterization was lately proposed by Pointin (1985). Since it was used with the model with 1.8km grid space, the horizontal pressure gradient effects were explicitly resolved in the model. It seems however, that in mesoscale models with grid resolution about 20 km, some characteristics of Pointin's approach would be desirable in order to account properly for the horizontal pressure gradient effects.

References

Anthes, R.A., 1977: A cumulus paramterization scheme utilizing a one-dimensional cloud model. Mon. Wea. Rev., 105, 270-286.

Barnes, G.M., and K. Sieckman, 1985: The environment of fast and slow moving tropical convective cloud lines. Mon. Wea. Rev., 112, 1782-1794.

Beniston, M., 1984: A numerical study of atmospheric mesoscale cellular convection. Dyn. Atmos. Oceans, 8, 223-242.

Cotton, W.R. and R.A. Anthes, 1986: Dynamic of clouds and precipitating mesosystems, Chapter X, Academic Press, to be published.

Frank, M.W. and C. Cohen, 1985: Properties of tropical cloud ensembles estimated using a cloud model and observed updraft population, J. Atmos. Sci., 42, 1911-1928.

Fritsch, J.M., and C.F. Chappell, 1980a: Numerical prediciton of convectively driven mesoscale pressure systems: Part I: Convective parameterization. J. Atmos. Sci., 37, 1722-1733.

Fritsch, J.M., and C.F. Chappell, 1980b: Numerical prediction of convectively driven mesoscale pressure systems. Part II: Mesoscale model. J. Atmos. Sci., 37, 1734-1762.

Gamache, J.F., and R.A. Houze, Jr., 1983: Water budget of a mesoscale convective system in the tropics. J. Atmos. Sci., 40, 1835-1850.

Holton, J.R., 1973: A one-dimensional cumulus model including pressure perturbations. Mon. Wea. Rev., 101, 201-205.

Landau, L.D. and E.M. Lifshitz, 1959: Fluid Mechanics, Pergamon Press, pp. 36.

LeMone, M.A., and E.J. Zipser, 1980; Cumulonimbus vertical velocity events in GATE. Part I: Diameter, intensity and mass flux. J. Atmos. Sci., 37, 2444-2457.

LeMone, M.A., 1983: Momentum transport by a line of cumulonimbus. J. Atmos. Sci., 40, 1815-1834.

LeMone, M.A., G.M. Barnes, and E.J. Zipser, 1984: Momentum flux by lines of cumulonimbus over the tropical oceans. J. Atmos. Sci., 41, 1914-1932.

Pointin, Y., 1985: Numerical simulation of organized convection. Part I: Model description and preliminary comparison with squall line observations. J. Atmos. Sci., 42, 155-172.

Raymond, D.J., 1984: A wave-CISK model of squall lines. J. Atmos. Sci., 41, 1946-1958.

Schneider, E.K., and R.S. Lindzen, 1976: A discussion of the parameterization of momentum exchange by cumulus convection. J. Geophys. Res., 81, 3158-3160.

Shapiro, L.J., and D.E. Stevens, 1980: Parameterization of convective effects on the momentum and vorticity budgets of synoptic-scale Atlantic tropical waves. Mon. Wea. Rev., 108, 1816-1826.

Stevens, D.E., 1979: Vorticity, momentum and divergence budgets of synoptic-scale wave disturbance in the tropical Eastern Atlantic. Mon. Wea. Rev., 107, 535-550.

Soong, S.-T., and W.-K. Tao, 1984: A numerical study of the vertical transport of momentum in a tropical rainband. J. Atmos. Sci., 41, 1049-1061.

Sui, C.-H., 1984: Cumulus effects on the large-scale vorticity and momentum fields in the tropical atmosphere. Ph.D. dissertation, University of California in Los Angeles.

Yanai, M., S. Esbensen, J.-H.Chu, 1973: Determination of bulk properties of tropical cloud clusters form large-scale heat and moisture budgets. J. Atmos. Sci., 30, 611-627.

Zipser, E.J., and M.A. LeMone, 1980: Cumulonimbus vertical velocity events in GATE. Part II: Synthesis and model core structure. J. Atmos. Sci., 37, 2458-2469.

Appendix A

The Formulation of the Convective Forcing Term in a Mesoscale Model

We discuss here some problems connected with the formulation of the convective forcing term in numerical models. We consider the horizontal momentum equation in the form:

$$\frac{du}{dt} = F \tag{A.1}$$

where u a horizontal velocity and F describes forcing (for example the horizontal pressure gradient). When the equation A.1 is used in the numerical model it has to be averaged over the grid volume. If we use anelastic approximation and write eq. A. 1 in the flux form we get:

$$\frac{\partial \bar{u}}{\partial t} = - \frac{\partial}{\partial x} (\bar{\bar{u}}\bar{\bar{u}}) - \frac{\partial}{\partial y} (\bar{\bar{u}}\bar{\bar{v}}) - \frac{\partial}{\partial z} (\bar{\bar{u}}\bar{\bar{w}}) - \frac{\partial}{\partial x} (\overline{u'u'}) - \frac{\partial}{\partial y} (\overline{u'v'}) -$$

$$\frac{\partial}{\partial y} (\overline{u'w'}) - \bar{w} \frac{1}{\rho o} \frac{\partial \rho o}{\partial z} + \bar{F} \tag{A.2}$$

where bar denotes the averaging operator it means for every variable X: $X = \bar{X} + X'$, and $\bar{X}' = 0$.

The goal of parameterization is usually to express eddy fluxes in terms of grid-scale values, or to find the expression for them from another, smaller scale model.

In the equation A.2 the horizontal eddy flux terms are generally assumed to be small compared to the vertical eddy flux terms. Horizontal eddy fluxes are usually parameterized in terms of grid-averaged variables and included in calculations for computational, rather then physical, purposes (Cotton and Anthes, 1986).

Now, let's consider the case when the subgrid-scale momentum flux is the result of convection. Our grid-averaged equation can be written now in the form:

$$\frac{\partial \bar{u}}{\partial t} = - \frac{\partial}{\partial x} (\bar{u}\bar{u}) - \frac{\partial}{\partial y} (\bar{u}\bar{v}) - \frac{\partial}{\partial z} (\bar{u}\bar{w}) - w \frac{1}{\rho o} \frac{\partial \rho o}{\partial z} + D + \bar{F} + F_c \qquad (A.3)$$

where D denotes horizontal eddy fluxes and F_c describes convective forcing involving vertical fluxes. F_c is usually calculated from the one-dimensional cloud model in the following manner (Yanai, 1973):

The grid area we consider, can be partitioned for the fractional area occupied by cloud (σ) and environment ($1 - \sigma$). For simplicity we neglect the downdraft. Now we can calculate u as:

$$\bar{u} = \sigma u_c + (1 - \sigma) u_E \qquad (A.4)$$

where the subscripts c and E denote cloud and environment respectively. In this case, the vertical derivative of the subgrid momentum flux can be expressed as (Yanai, 1973):

$$F_c = - \frac{\partial}{\partial z} [\sigma(1 - \sigma)(u_c - u_E)(w_c - w_E)] \qquad (A.5)$$

when the area of the cloud σ is small F_c can be approximated as:

$$F_c = - \frac{\partial}{\partial z} [\sigma w_c (u_c - u_E)] \qquad (A.6)$$

Expression A.6 is usually used as the convective forcing term in the momentum equation aveaged over the grid scale and u_c and w_c are calculated from the one-dimensional cloud model. Horizontal velocity in the environment u_E is usually assumed to be equal to $\bar{u}$ (eq. A.4, with $\sigma << 1$ and $u_c \sim u_E$) and is calculated in the mesoscale (or large-scale) model.

Fritsch and Chappell (1980 a, b) calculate convective forcing using a different method. In their approach the convective forcing term is equal to:

$$F_c' = \left.\frac{\partial \bar{u}}{\partial t}\right|_{cloud} = \frac{\bar{u}_F - \bar{u}_o}{\tau} \qquad (A.7)$$

where $\left.\frac{\partial u}{\partial t}\right|_{cloud}$ denotes the local change in the mean momentum calculated from the cloud model. $\bar{u}_o$ is equal to the horizontal velocity in the grid area before the parameterization, τ is the characteristic time for convection (see chapter II) and $\bar{u}_F$ is the horizontal velcoity in the grid volume after the parameterization. $\bar{u}_F$ is calculated according to the formula A.4. Horizontal velocity in clouds u_c is calculated from the cloud model and u_E is equal to:

$$u_E = u_o + \int_o^\tau - w_E \frac{\partial \bar{u}(t)}{\partial z} \, dt \qquad (A.8)$$

where w_E is the vertical velocity in the environment and is calculated from the eq. 3.1.

Our results for the convective lines show (Fig. A-1) that the convective forcings calculated from eq. A.6 and A.7 differe substantially when the average vertical velocity is different then zero. Our explanation why this is the case is the following:

In calculations of the horizontal momentum after the parameterization - $\bar{u}_F$, the mean values of u and w are not subtracted. It means that $\frac{\partial \bar{u}}{\partial t}\Big|_{cloud}$ calculated from the formula A.7 containes not only eddy but also mean advective terms i.e.:

$$F_c' = \frac{\partial \bar{u}}{\partial t}\Big|_{cloud} = -\frac{\partial}{\partial z}(\overline{uw}) = -\frac{\partial}{\partial z}(\bar{\bar{w}}\bar{\bar{v}}) - \frac{\partial}{\partial z}(\overline{u'w'}) \qquad (A.9)$$

Fig. A-1 shows that it is really the case. When expression give by F_c' is put into the averaged equation A.2 as a convective forcing the advective term $-\frac{\partial}{\partial z}(\bar{\bar{u}}\bar{\bar{w}})$ is accounted for twice.

Therefore, we conclude that the formula A.6 is not a proper expression for the convective forcing. The convective forcing should be calculated either directely as a momentum flux derivative (eqs. A.5, A.6)) or, when local derivatives produced by a cloud model are used, vertical advection by the mean wind has to be subtracted (the last approach was used for example by Pointin, 1985). It is worth mentioning, that no matter which approach is used it is the eddy flux term that needs to be parameterized. The same kind of reasoning can be applied when three-dimensional cloud model is used. In this case, if local derivatives produced by cloud model $\frac{\partial u}{\partial t}\Big|_{cloud}$ are used in calculation of the convective forcing, F_c should have the form.

$$F_c = F_c' + \frac{\partial}{\partial z}(\bar{\bar{u}}\bar{\bar{w}}) + \frac{\partial}{\partial x}(\bar{\bar{u}}\bar{\bar{u}}) + \frac{\partial}{\partial y}(\bar{\bar{u}}\bar{\bar{v}}) =$$

$$= \left.\frac{\partial u}{\partial t}\right|_{\text{cloud}} + \frac{\partial u}{\partial z}\,(\bar{u}\bar{w}) + \frac{\partial}{\partial x}\,(\bar{u}\bar{u}) + \frac{\partial}{\partial y}\,(\bar{u}\bar{v}) \qquad \text{(A.10)}$$

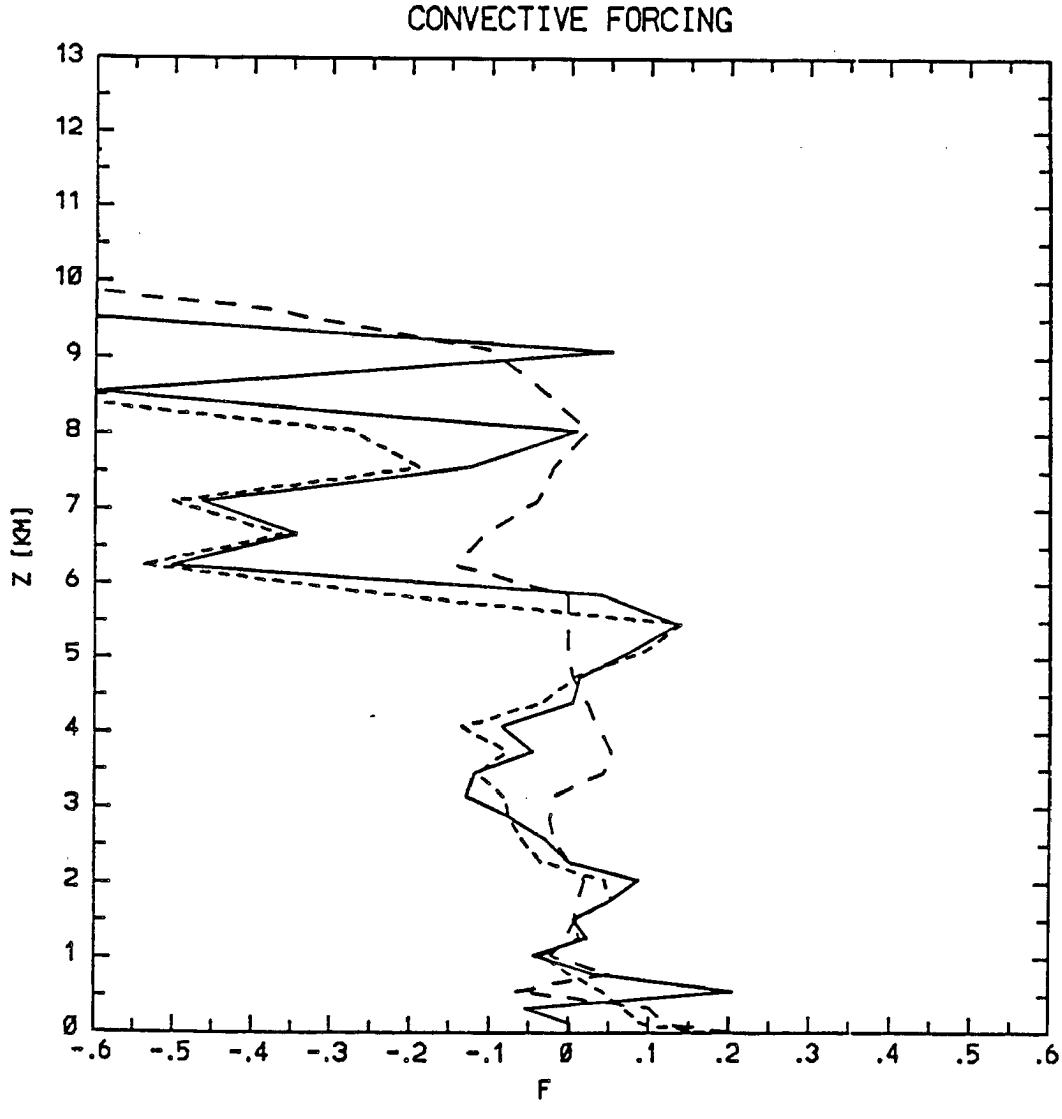

Fig. A-1 The comparison of the convective forcing calculated from the formula A.5 and A.6. The solid line indicates the momentum flux derivative $\frac{\partial}{\partial z}$ (u'w') the dashed line the convective forcing calculated according to the eq. A.6 ($-\frac{\partial \bar{u}}{\partial t}$ cloud), the fine dashed line indicates $-\frac{\partial u}{\partial t}$ cloud $-\frac{\partial}{\partial z}(\overline{uw})$.

Appendix B

Virtual Mass Effect

When we consider the movement of a body in fluid under the influence of an external force, the equation of motion is given by:

$$M \frac{d\underset{\sim}{u}}{dt} + \frac{d\underset{\sim}{p}}{dt} = \underset{\sim}{f} \qquad \text{B.1}$$

where $\underset{\sim}{f}$ is the external force, $\underset{\sim}{P}$ is the momentum of the fluid and $M\underset{\sim}{u}$ is the momentum of the body. It can be shown (see for example Landau, and Lifshitz, 1959) that the components of the fluid momentum can be written as:

$$P_i = m_{ik} u_k \qquad \text{B.2}$$

where m_{iK} is called an induced mass tensor. Using the formula B.2 we can write the equation of motion in the form:

$$\frac{du_K}{dt} (M\delta_{ik} + m_{ik}) = f_i \qquad \text{B.3}$$

Obtaining the induced mass coefficient for a given body is, in general, a complicated procedure and requires solving the flow of the fluid past the body with proper boundary conditions (for further details see Landau and Lifshitz, 1959).

In atmospheric science the induced mass concept is usually used in one dimensional Lagrangian cloud models (for example: Anthes,

1979; Frank and Cohen, 1985). Since the vertical momentum equation for a buoyant parcel predicts vertical velocities larger than those actually observed, the density of the parcel in the vertical momentum equation is increased by a factor $(1 + \alpha)$, where α is called an virtual mass coefficient. Usually it is assumed that $\alpha = .5$ what corresponds to the induced mass calculated for the potential, incompressible flow passing a spherical body. In reality calculation of an induced mass tensor for the buoyant parcel would be practically impossible. Introducing the virtual mass parameter ($\alpha = .5$) in the vertical momentum equation results from the need for fitting the calculated vertical velocity to observations, rather than from detailed theoretical consideration. Therefore following Anthes (1979), we use $\alpha = .5$ in the vertical momentum equation but we assume that $\alpha = 0$ in the horizontal momentum equation. From the sensitivity tests for the Lagrangian parcels described in Chapter IV, we estimated that including $\alpha = .5$ in the horizontal momentum equation decreases the average momentum flux for the Lagrangian parcels about 15% - 20% at 6 km (where the change of momentum due to the change of α is the largest). Assuming $\alpha = 0$ in the vertical momentum equation causes about a 15% increase in the vertical velocity and a slight increase in the momentum flux.